UPPSALA
UNIVERSITET

Emerging Roles of the nuclear polyadenylate binding protein PABPN1 as a regulator of nuclear export of human adenovirus RNA

Name: Katharina Julia Kases

Master Degree Project in Infection Biology, 30 credits. Summer 2021
3MK007
Department: Medical Biochemistry and Microbiology
Supervisor: Assoc. Prof. Dr. Tanel Punga

Table of Contents

Abstract

Human adenovirus is a well characterised DNA virus that exhibits a fascinatingly complex genome regulation. Indeed, the viral major late transcription unit (MLTU), producing transcripts during late phases of infection, harbours a multitude of alternative polyadenylation, and splicing acceptor sites, giving rise to a vast array of viral RNAs. The control of alternative polyadenylation (APA) site activity is an intricate, yet broadly studied process, employing various cis- and trans-acting factors. The nuclear polyadenylate protein, PABPN1, has been identified as one such trans-acting factor. Previous reports described PABPN1 as a regulator of polyadenylation, transcript decay, nuclear export of mature mRNAs, and as an unexpected regulator of transcription under certain circumstances. Here, PABPN1 reveals to have a role in human adenovirus C5 (HAdV-5) infections. Immunofluorescence microscopy visualised a distinct change in subnuclear localisation of PABPN1 in infected A549 cells. Knockdown experiments indicate that PABPN1 affects certain late transcripts on both RNA and protein level, while early transcripts remain unaffected. Depletion of PABPN1 from infected cells decreased cytoplasmic protein VI specifically, whereas other virus and host control proteins did not exhibit any impact. Analysis of polyadenylate tails of viral RNAs transcribed from the MLTU highlights the varying activity of PABPN1 on different polyadenylation sites. Furthermore, when cytosolic and nuclear virus RNA extracts were compared, PABPN1 depletion revealed to cause partial accumulation of MLTU transcripts within the nucleus. This effect could not yet be fully explained, however, preliminary data obtained from 4sU-labelled RNA, suggests that PABPN1 could act as a negative regulator of virus transcription.

Popular Science Summary

The Central Dogma of Biology

Every living organism owns a “blueprint” that enables their cells to grow and to divide. This “blueprint” is our DNA which is used to make RNA. RNA in turn, is used to make proteins. Proteins have many functions, for instance modifying their own “blueprint”, the RNA. This activity has different outcomes: e.g. the amount of RNA can be changed or the RNA localisation within the cell might become different. The way how RNA is modified depends on the protein, its environment and when it becomes active. One such environment can be a virus infection, e.g. with adenovirus that causes “common cold”, diarrhoea or eye infections.

Background of this Study

Viruses are parasites that need our cells and proteins to help their replication and spread. One of these human proteins is called PABPN1. Not a lot is known about this protein, but we know that it belongs to the family of RNA-regulating proteins. This is important as the adenovirus can manipulate PABPN1 to help its replication and thereby support the virus infection. Studying this protein in virus infected cells *in vitro* (in the lab) helps us to better understand both the virus itself and the protein’s function. If PABPN1 is important to this virus, it might be important for other, worse pathogens too.

Methods and Results

In vitro experiments allow to compare the behaviour of human proteins naturally, and in virus infection. In adenovirus infection, PABPN1 changes its localisation within the cell, implying that PABPN1 is indeed important to the virus. Furthermore, studying the “blueprint”, RNA, showed that the regulatory protein PABPN1 modifies the length of viral RNAs specifically. These modifications have different implications for the behaviour of viral RNA. Most importantly, such changes can affect how many proteins can be made, or how well the virus can replicate within the cell.

Why is studying RNA and proteins important?

Studying how virus RNA is selectively changed by human proteins during virus infection helps to explain how viruses manipulate our cells to help with their replication. By identifying a human protein that is very important to the virus but not so important to us (because other proteins can substitute its function), we can find a potential drug target. This means that we ourselves can then manipulate the protein that has been studied, so that it can no longer help the virus during infection. This is especially important if the protein we are studying is not only useful for adenovirus but also for other, maybe worse pathogens.

Introduction

Human adenovirus harbours multiple polyadenylation sites

Adenoviruses are nuclear replicating viruses, possessing double-stranded DNA genomes that comprise ten different transcription units categorised into early, intermediate or late temporal classes, relative to the onset of DNA replication (Thomas and Mathews, 1980). Transcripts of the early class consist of E1a, E1b, E2, E3 and E4, whereas Iva2, pIX and L4 transcripts constitute the intermediate class (Fessler and Young, 1998; Leong and Berk, 1986). The transition to late gene expression is dependent on viral DNA replication as well as an anti-termination activity of RNA polymerase II (RNAP II). The loss of the obligatory first polyadenylation site usage (anti-polyadenylation) during late phase virus infection allows RNAP II to proceed into the major late transcription unit (MLTU) region without undergoing upstream displacement (Falck-Pedersen and Logan, 1989; Shaw and Ziff, 1980; Thomas and Mathews, 1980).

The MLTU, whose transcription is driven by the major late promotor (MLP), comprises transcripts for mainly structural proteins, which are assigned to the RNA families L1 to L5, dependent on the usage of alternative polyadenylation sites (Figure 1A). RNA families are further divided into multiple RNA species based on the use of a variety of splicing acceptor sites found within the MLTU (Falck-Pedersen and Logan, 1989) (Figure 1B). Downstream of the MLP the 5' tripartite leader (TPL) is located, constituted by three non-coding exons (1 to 3), and functioning as translational enhancer element after splicing. The TPL is infrequently interspersed by the i-leader (located between TPL exons 2 and 3), which codes for the i-leader protein (Figure 1A) (Logan and Shenk, 1984). Further 5' leader sequences, present to varying degrees on a subset of MLTU RNAs, are denoted x-, y- and z-leaders. Thus, the diversity exhibited by mRNAs encoded by the MLTU are by virtue of the combination of varying 5' UTRs, multiple splicing variants and varying 3' UTRs through alternative polyadenylation activity (Chow and Broker, 1978; Ramke et al., 2017).

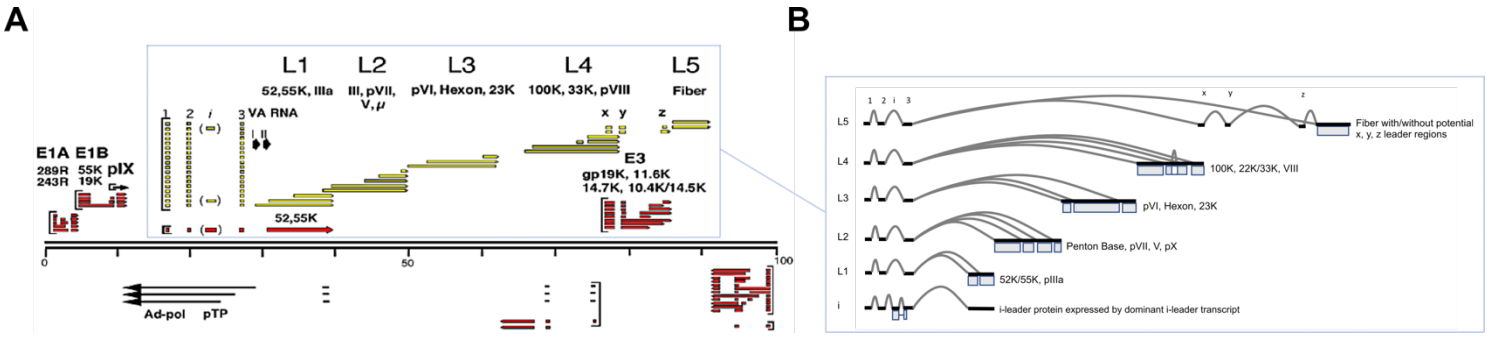

Figure 1. Overview of adenovirus transcription and splicing maps. A. The classical illustration of the human adenovirus type 5 transcript map by Akusjärvi (2010). Forward transcripts are encoded by the top strand and transcribed in the direction of left to right, while reverse transcripts are encoded by the bottom strand and transcribed in the direction of right to left. Squared brackets indicate conventional transcription start sites (TSS). Adenovirus gene expression is categorised into early, intermediate and late phases in relation to the onset of DNA replication. Red-coloured transcripts belong to the class of early genes, whereas yellow-coloured transcripts constitute late genes. Intermediate class transcripts are illustrated as black arrows. **B.** Depicted are splicing events specific to individual MLTU L1 to L5 mRNAs, as well as the i-leader protein (Donovan-Banfield et al, 2020). Splicing events (grey lines) of exons (black lines) place the AUG of each major ORF (boxes) immediately downstream of tripartite leader exons (TPL; 1, 2, 3).

Multi-level regulatory mechanisms of alternative polyadenylation

The occurrence of not solely one but multiple polyadenylation (polyA) sites on human genes is a widespread phenomenon, which can also be observed on the adenovirus MLTU. Therefore, processing of the 3' end of mRNAs has to be controlled by an intricate regulatory mechanism, producing an array of transcript isoforms defined by alternative (cleavage) and polyadenylation (APA). In principle, cleavage and polyadenylation is regulated through the highly conserved, canonical polyadenylation signal (PAS) AAUAAA located 5' of the cleavage site, and less conserved GU- or U-rich downstream sequence elements (DSEs) found 3' of the cleavage site. However, five further mechanisms of APA control have been proposed. Indeed, regulation of 3' end processing is generally considered to be controlled by chromatin structure, transcription, splicing, 3' end processing factors, and trans-acting factors (reviewed by Elkon et al., 2013).

Interestingly, polyadenylation has been described to be subjected to epigenetic modification through the depletion of nucleosomes on DNA coding for polyadenylation sites, whereas regions downstream of the encoded polyA site are enriched in nucleosomes. Furthermore, polyA sites encoded by genes harbouring multiple possible polyA sites exhibit stronger depletion of nucleosomes, whereas downstream regions reveal stronger enrichment of nucleosomes. The interaction between components of the transcription and of the 3' processing machinery has been reported to increase cleavage efficiency, thereby aiding the preferential the usage of proximal polyA sites during polyadenylation events. Furthermore, a positive correlation between elevated transcriptional activity and cleavage at proximal polyA sites has been described. Pre-mRNA processing represents another factor implied in APA regulation, based on the interaction of cleavage and polyadenylation factors at terminal introns of pre-mRNA causing increased cleavage of polyA sites located at the 3' UTR (reviewed by Elkon et al., 2013). The PAS AAUAAA and GU-/U-enriched DSEs provide cis-regulatory signals recognised and bound by 3' end processing factors, such as cleavage and polyadenylation specificity factors (CPSFs) and cleavage stimulation factors (CSTFs), respectively (Mann et al., 1993; Prescott and Falck-Pedersen, 1994; Takagaki and Manley, 1997). A negative correlation between the expression activity of 3' end processing factors and the 3' UTR length of mRNAs has been proposed. Trans-regulators comprise RNA-binding proteins (RBPs) binding in close proximity to intronic or 3' UTR polyA sites, and thereby influence cleavage activity of these sites. The nuclear polyadenylate binding protein PABPN1 (Figure 2C) has been reported to associate with proximal polyA sites whereby their cleavage becomes repressed, thus cleavage and polyadenylation occurs at distal polyA sites instead (de Klerk et al., 2012; Elkon et al., 2013 (review); Jenal et al., 2012).

APA regulation of adenovirus MLTU transcripts

RNAs produced from adenovirus MLTU are evidently subjected to aforementioned regulation of 3' UTR processing. However, further notice should be taken of following regulatory events. While the transition from early to late gene expression is dependent on DNA replication (Falck-Pedersen and Logan, 1989; Shaw and Ziff, 1980; Thomas and Mathews, 1980), the activity of polyadenylation sites present on the MLTU is controlled by a more intricate mechanism. As suggested by Mann et al. (1993), the initial polyadenylation site found on L1 RNA can be assumed to exhibit lower efficiency, eventually allowing for the usage of downstream polyA sites of L2 to L5 RNAs. Further, the interaction between CPSF and the PAS AAUAAA is comparatively unstable in the absence of CSTF. Association of CSTF to RNA-bound CPSF generally increases the overall stability of the 3' end processing complex. Nevertheless, complex stability varies dependent on the MLTU transcript. While the proximity of the L1 RNA polyA site to the transcription machinery provides a selective advantage for polyadenylation events, the CPSF/CSTF complex has been reported to be more stable when associated to L3 RNA. Polyadenylation of L2 to L5

RNAs is further aided by the decrease of CSTF, resulting in dissociation of less stable processing complexes (Mann et al., 1993). Adenovirus MLTU transcripts harbour APA sites to varying degrees. L1 has been described to possess four distinct polyA sites, whereas solely a singular polyadenylation site has been identified on L2 RNA as of yet. L3 and L4 reveal to harbour two polyA sites each, while there are six polyA sites presently found on L5 RNA (Moullec et al., 1983; Prescott and Falck-Pedersen, 1994; Zhao et al., 2014).

PABPN1 as a versatile regulator of polyadenylation, mRNA decay, and nuclear export

As aforementioned, PABPN1 has been identified as a trans-acting factor, regulating polyadenylation through its interaction with subunits of the CPSF and CSTF complexes, and the polyadenylate polymerase (PAP). Briefly, co-transcriptional association of PABPN1 and the CPSF complex to nascent RNA results in the synergistic interaction between PABPN1 and CPSF complex, stimulating the polyadenylation activity of PAP. In the absence of both 3' end processing factors, PAP exhibits low affinity for RNA, whereas presence of PAPBN1 and the CPSF complex induces high processivity at the 3' end of RNA until the polyA tail has reached a length of 200 to 300 nucleotides (Bresson and Conrad, 2013; Kühn et al., 2009). Thereafter, the distance between the initial CPSF binding site and current distal location of the polyadenylation complex, combined with a change in PABPN1 conformation (association into filamentous structures along the polyA tail; Figure *2*A) have been proposed to result in the dissociation of the CPSF complex, thereby reducing the affinity of PAP for RNA. Hence, processive polyadenylation is halted, while distributive polyadenylation remains stimulated by PABPN1 (Jenal et al., 2012; Kühn et al., 2009; Wahle, 1995).

Polyadenylate tail length control is a crucial step in 3' end processing as the length of the polyA tail can determine the fate of mRNAs within the nucleus. Importantly, polyA tail length has been identified as a one factor regulating the nuclear export of processed, mature mRNAs (Fuke and Ohno, 2008; Palazzo and Lee, 2018 for review). Export of transcripts by the nuclear pore complex (NPC) has been coupled to post-transcriptional 3' processing in a PABPN1-dependent manner through its interaction with ALYREF, a subunit of the TREX (transcription and export) complex (Shi et al., 2017) (**Figure *2***A). Further, polyA tails that are too short as well as hyperadenylated tails equally are subjected to exosome-mediated decay. The human PABPN1 and its yeast homologue Pab2p, exclusively present in Schizosaccharomyces pombe, have been reported to physically associate to the exosome complex (Figure *2*B). These findings indicate nuclear RNA degradation to be regulated by cis- and trans-acting factors, namely the polyA tail length and PABPN1-dependent recruitment of the exosome, respectively (Beaulieu et al., 2012; Bresson and Conrad, 2013; Meola et al., 2016).

Despite its well-established role in the regulation of post-transcriptional polyadenylation events, a more unexpected function of PABPN1 as a putative regulator of transcription has been proposed. PABPN1 has been described to associate to RNAP II before or shortly after transcription initiation, implicating a role in transcriptional regulation, independent of its 3' end processing regulatory activity (Bear et al., 2003). Exceptionally, Kim et al. (2001) demonstrated PABPN1 to interact with Ski-interacting protein (SKIP), associating to the E-box motif resulting in the enhancement of MyoD transcription. SKIP itself has been implied as a positive regulator of TGF-β (transformation growth factor β) (Leong et al., 2001), known as a target of various RNA and DNA viruses, either stimulating or repressing the progression of the viral infection (Denney et al., 2018; Dickinson et al., 2020; Hancock et al., 2020; Nanbo et al., 2018).

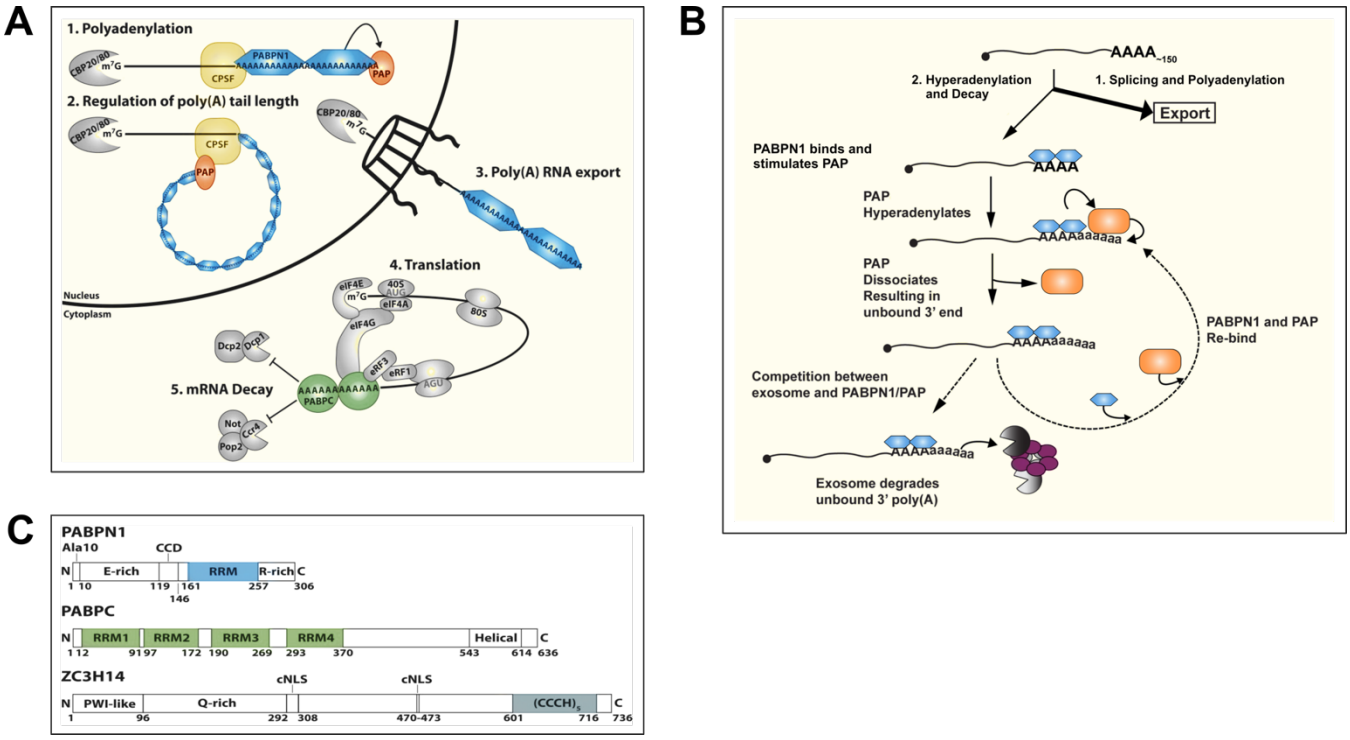

Figure 2. PABPN1 is a multifaceted regulator of polyadenylation, mRNA decay and nuclear export. A. PABPN1 regulates polyA tail length through its association to adenosines, generating a filamentous structure, thereby disrupting the interaction between the polyadenylate polymerase (PAP) and the CPSF complex when 200 – 300 nucleotides have been added to the 3' end of the mRNA. Thus, PAP changes from processive activity to distributive activity. **B.** PABPN1 exhibits bimodal activity. (1.) PABPN1 acts as a positive regulator of transcript processing through stimulation of polyadenylation associating to the CPSF complex and PAP. (2.) PABPN1 induces hyperadenylation through PAP, generating polyadenylate tails of aberrant length. RNA decay is mediated by the exosome complex, recruited by deviating polyA tail lengths as well as physical interaction with PABPN1. **C.** Overview of three well-studied RNA-binding proteins (RBPs). The nuclear polyadenylate binding protein PABPN1 harbours one RNA recognition motif (RRM), while its cytoplasmatic counterpart PABPC1 possesses four RRMs. Human ZC3H14 is the homologue of the extensively-described yeast Nab2 (*S. cerevisiae*), mediating RNA interaction through the C-terminal zinc finger motif. Panels A and C are adapted from Wigington et al. (2014). Panel B is adapted from Bresson et al. (2013).

PABPN1 has an emerging role in virus infections

The cytoplasmic counterpart of PABPN1, PABPC2 (Figure 2C), has been described as a "common target" in virus infections (Smith and Gray, 2010 for review), similarly to TGF-β. While picornaviruses cleave PABPC1, disrupting the interaction of PAPBC1 with eIF4G during translation initiation and thereby inhibiting efficient host protein synthesis. Human cytomegalovirus (HCMV), Dengue virus and vaccinia virus recruit PABPC1 to virus transcripts to enhance translation of viral proteins (reviewed by Smith and Gray, 2010). However, few reports have addressed PABPN1 as a target in virus infections (Chen, 1999; Salaun et al., 2010).

Aims

Partly based on the aforementioned elusive nature of the PABPN1 protein, hinting at its functional versatility, and partly inspired by the recently published article by Donovan-Banfield et al. (2020), once more highlighting the intricacy of the polyadenylation events occurring at the adenovirus MLTU (already well described by Zhao et al. (2014)), it was sought to establish the role of this nuclear polyadenylate binding protein in human adenovirus infections. Overall shortening of late transcripts has been reported, similar to behaviour of RNAs observed in coronavirus infections, as well as a dissonance between transcriptional activity and protein abundance (Donovan-Banfield et al., 2020). Thus, following aims were formulated: (1) establishment of the effect of PABPN1 on protein levels, based on its influence on adenovirus MLTU transcript abundance (2), (3) observation of activity dependent on the alternative polyadenylation sites present on MLTU, as well as its role in transcript stability (4).

Material and Methods

Cell Culture and Virus Infection

Adenocarcinomic human alveolar basal epithelial cells A549 were maintained in culture media (Dulbecco's Modified Eagle's Medium (DMEM), 10 % foetal calf serum (FCS), 0.02 U/mL penicillin, 0.02 µg/mL streptomycin (Thermo Fisher Scientific)). Standard growth conditions comprised a humidified atmosphere of 37 °C supplied with 5 % CO_2. Human adenovirus type 5 (HAdV-5) used for infections in this study was purified by Dr. R. T. Inturi (Uppsala University, Uppsala, Sweden). Cells were treated with siRNA for 24 hours, thereafter the culture media was changed, and cells were exposed to HAdV-5 for one hour at a multiplicity of infection (MOI) of 5 or 10 (5 or 10 FFU/cell) in DMEM supplemented with 10 % newborn calf serum (NCS). Unbound virus remaining within the supernatant was removed by washing cells with culture media.

Knock-down of RNA-binding proteins by siRNA

Scramble siRNA negative control (MWG Operon, 47% GS content control siRNA (siScr)), MKRN2, PABPN1 and CPSF1 siRNA (Thermo Fisher Scientific) were introduced into cells at a final concentration of 45 nM using jetPRIME reagent (Polyplus Transfection) according to the manufacturer's protocol. To establish the effect knock-down respective proteins had on HAdV-5 major late transcription unit (MLTU) transcripts and corresponding proteins, siScr control, siMKRN2-, siPABPN1- and siCPSF1-treated cells were infected at MOI 10 at 24 hours post-transfection (hpt). At 24 hours post-infection (hpi) whole cell lysates were obtained by lysis with 1 × radio-immunoprecipitation assay buffer (RIPA) and subsequent soniciation (5 to 10 cycles at high settings, alternating between 30 seconds on and 30 seconds off; Bioruptor, Diagenode). Proteins were separated by SDS-PAGE and detected by western blotting.

Indirect Immunofluorescence Assay

Cells grown on 15 mm coverslips (Thermo Fisher Scientific), subjected to 24 hours of siRNA treatment, followed by 24 hours HAdV-5 infection were fixed with 1.5 % paraformaldehyde in PBS for 15 minutes at room temperature. Subsequently, cells were permeabilised with a solution of PBS – Triton X-100 (0,1 %) for 15 minutes at room temperature. Non-specific antibody binding was blocked with a PBS-based solution (22.52 mg/mL L-glycine; 1 % BSA; 0,1 % Tween-20) at room temperature for 30 to 45 minutes. Samples were incubated with primary antibodies (1:1.000 dilution) under humidified conditions either up to 2 hours at room temperature or at 4 °C overnight. To visualise targeted proteins, samples were incubated with secondary antibodies (1:2.000 dilution) conjugated to fluorescent dyes Alexa Fluor 488 or Alexa Fluor 594 (Alexa Fluor, Abcam) (Table 1) for up to one hour at room temperature in the dark. Visualisation of the nucleus was achieved by staining DNA with 300 nM DAPI for 3 to 5 minutes at room temperature in the dark. In between each staining step samples were washed thrice, up to 10 minutes in total, with solutions of PBS or PBS containing 0,1 % Tween-20 and 1 % BSA. Fixed cells were preserved in ProLong mounting reagent (Thermo Fisher Scientific), and visualised by epifluorescence microscopy (Eclipse 90i, Nikon).

Table 1. Primary and secondary antibodies

Primary Antibodies	Manufacturer
anti-pV (rabbit IgG)	David Matthews, personal communication
anti-pVI (mouse IgG)	Harald Wodrich, personal communication
anti-pVII (mouse IgG)	Harald Wodrich, personal communication
anti-72K (rabbit IgG)	Bruce Stillman, personal communication
anti-L4-100K (rat IgG)	Thomas Dobner, personal communication
anti-MKRN2 (rabbit IgG)	Sigma (SAB2101484)
anti-PABPN1 (rabbit IgG)	Abcam (ab75855)
anti-PABPN1 (mouse IgG)	Proteintech (66807-1-IG)
anti-CPSF1 (mouse IgG2b)	Santa Cruz Biotechnology (sc-166281)
anti-Actin (goat IgG)	Santa Cruz Biotechnology (sc-1616)
anti-GAPDH (rabbit IgG)	Santa Cruz Biotechnology (sc-47724)
anti-Histone 3 (rabbit IgG)	Abcam (ab18521)
anti-Tubulin (rabbit IgG)	Santa Cruz Biotechnology
Secondary Antibodies	**Manufacturer**
Donkey anti-mouse IgG	LI-COR (926-68072)
Goat anti-mouse IgG1	LI-COR (926-32350)
Goat anti-mouse IgG2b	LI-COR (926-32352)
Donkey anti-goat IgG	LI-COR (926-32214)
Goat anti-rabbit IgG	LI-COR (926-68071)
Goat anti-rat IgG	LI-COR (926-68076)

Fractionation of Cellular Compartments

After 24 hours of siRNA treatment and subsequent 24 hours of HAdV-5 infection, cells were subjected to one of three fractionation approaches evaluated in this study.

Ambion Protein and RNA Isolation System (PARIS) Kit (Invitrogen, Thermo Fisher Scientific)

Cellular contents were separated into cytosolic and nuclear fractions according to the manufacturer's protocol. Deviations from the protocol included removal of 20 % of the lysates obtained subsequent to disruption of the plasma membrane for isolation of total RNA. Furthermore, 7 % of each the cytosolic and the nuclear fractions was removed for western blot analysis. TRIzol LS Reagent (Thermo Fisher Scientific) was added according to a ratio of 3:1 to samples allotted to RNA isolation. Samples were stored at -20 °C until the RNA isolation.

Rapid, Efficient and Practical (REAP) assay (Suzuki et al., 2010)

Cellular contents were separated into cytoplasmic and nuclear fractions according to Suzuki et al. (2010). Briefly, cells grown as a monolayer on 100 mm cell culture dishes (approximately to 70 – 80 % confluency) were washed with 1 × PBS, and collected by scarping cells into PBS. Cells were pelleted through "pop-spin" (up to 10.000 × g) for 10 to 15 seconds at 4 °C. The supernatant was removed and pellets resuspended in 900 µL in a solution of PBS, 0,1 % NP-40 (1 × PBS, 0,1 % w/v Igepal CA-360). Suspen-

sions were triturated 7 times with a P1000 pipette to lyse the plasma membrane. One third of the lysate was removed and distributed 1,5:1 for subsequent total RNA isolation and western blot analysis. Samples were kept on ice until further processing. The remaining lysate was centrifuged for 10 seconds ("pop-spin") at 4 °C to separate the cytoplasm from the nuclear pellet. Half of the supernatant containing the cytoplasmic fraction was removed and distributed 1,5:1 for subsequent cytoplasmic RNA isolation and western blot analysis. Samples were kept on ice until further processing. The remaining supernatant was discarded and the nuclear pellet was washed with 900 µL PBS, 0,1 % NP-40. Suspensions were centrifuged for 10 seconds ("pop-spin") at 4 °C, and the supernatant was removed. Nuclear pellets were resuspended in 300 µL 1 × RIPA buffer, and the nuclear fraction was distributed 1,5:1 for subsequent nuclear RNA isolation and western blot analysis. TRIzol LS Reagent was added according to a ratio of 3:1 to samples allotted to RNA isolation, and samples were stored at -20 °C until the RNA isolation.

Cell Fractionation Kit - Standard (Abcam)
Cellular contents were separated into cytosolic and nuclear fractions mainly following the manufacturer's protocol. Prior to the fractionation procedure, the volumes of the cell suspensions allotted to fractionation, to isolation of total RNA, and to western blot analysis were determined. Subsequently, equal volumes were allotted to isolation of cytosolic and nuclear RNA, respectively, as well as to western blot analysis of cytosolic and nuclear fractions. Additional washing steps while separating cytosolic and nuclear fractions were introduced to increase the purity of respective fractions. The cytosolic fraction was centrifuged for one minute at 10.000 × g and 4 °C, the supernatant transferred to new tubes, and additionally centrifuged for 5 minutes at 13.000 × g and 4 °C. The nuclear pellet was washed with Buffer A, repelleted for 2 minutes at 5.000 × g and 4 °C, and resuspended in 1 × RIPA buffer. Samples were lysed for 30 minutes on ice. TRIzol LS Reagent was added according to a ratio of 3:1 to samples allotted to RNA isolation, and samples were stored at -20 °C until the RNA isolation.

All samples containing protein for western blot analysis, obtained by different fractionation methods, were kept on ice or at -20°C until they were subjected to 5 to 10 cycles of sonication, high settings, alternating between 30 seconds on and 30 seconds off (Bioruptor, Diagenode).

RNA Isolation

RNA Isolation by TRI Reagent (Sigma-Aldrich)
Total RNA was isolated from cells according to the manufacturer's protocol. Reaction volumes were reduced by 50 % to accommodate for lower cell counts on 35 mm or 60 mm culture dishes. To increase RNA yields, RNA was precipitated at -20 °C overnight, and pelleted for 15 minutes at 12.000 × g and 4 °C. RNA was reconstituted in 30 to 50 µL of sterile water, depending on the anticipated RNA yield. To facilitate reconstitution RNA pellets were incubated at 60 °C for up to 5 minutes.

RNA Isolation by TRIzol LS Reagent (Thermo Fisher Scientific)
RNA was isolated from fractionated samples following the manufacturer's protocol. To increase yields, samples were vortexed up to 3 minutes during respective incubation steps at room temperature, and RNA was precipitated at -20 °C overnight with the addition of 1 µL glycogen. The centrifugation time pelleting RNA was increased up to 20 minutes at 12.000 × g and 4 °C. RNA was reconstituted in 30 to 50 µL of sterile water. To facilitate dissolution RNA pellets were incubated at 60 °C for up to 5 minutes.

RNA Isolation with Phenol/Chloroform

Cells grown on 60 mm culture dishes (80 to 100 % confluency), were washed with 1 × PBS, lysed with 600 µL isoB – NP-40 solution (10 mM Tris pH 7,5; 0,15 M NaCl; 1,5 mM $MgCl_2$; 0,65 % w/v NP-40) and transferred into tubes. Samples were vortexed for 20 seconds and incubated on ice for 5 minutes. Lysates were centrifuged for 3 minutes at 11.500 × g and 4 °C, and the supernatant transferred to new tubes. 130 µL 5 × RPS (1 M Tris pH 8,8; 10 % w/v SDS, 1% w/v EDTA) and 600 µL phenol were added to the supernatant. Samples were vortexed for one minute and centrifuged for 5 minutes at 13.000 × g and 4 °C. The aqueous phase was transferred to new tubes, and equal volumes of phenol were added. Samples were vortexed for one minute and centrifuged for 5 minutes at 13.000 × g and room temperature. The aqueous phase was transferred to new tubes and equal volume of a chloroform – isoamyl alcohol (4 % v/v) solution were added. Samples were vortexed for one minute and centrifuged for 5 minutes at 13.000 × g and room temperature. The aqueous phase was transferred to new tubes and 600 µL isopropanol, 1 µL glycogen and 122 mM NaCl were added. Samples were vortexed and RNA precipitated at -20 °C overnight. RNA was pelleted for 30 minutes 13.000 × g and 4 °C. Pellets were reconstituted in 50 µL sterile water.

Reverse Transcription of RNA into cDNA

Prior to reverse transcription, RNA was treated with DNAse (RapidOut; Thermo Fisher Scientific) according to the manufacturer's protocol. Depending on RNA yields, between 40 ng up to 1 µg RNA were reverse transcribed by SuperScript III Reverse Transcriptase (Invitrogen, Thermo Fisher Scientific) following the manufacturer's protocol. Random primers were added to a final concentration of 250 nM per reaction. The recommended RNAseOut Recombinant RNAse Inhibitor was substituted by equal volumes of sterile water. Reaction volumes were reduced by 50 % when suitable. The adapted PCR protocol comprised incubation for 5 minutes at 25 °C, subsequent incubation for one hour at 52 °C, and inactivation for 15 minutes at 70 °C. cDNA was diluted between 1:5 up to 1:10 to suitable concentrations of 1 – 5 ng/µL, depending on the initial amount of RNA used.

Analysis of Fractionation Experiments by Agarose Gel Electrophoresis

cDNA generated from RNA isolated during fractionation procedures was incubated with primers targeting human $tRNA^{lys}$ and MALAT1, cytosolic and nuclear RNA controls, respectively. PCR reactions were carried out with the addition of 3 % DMSO according to the Phire Hot Start II DNA Polymerase protocol (Thermo Scientific, Thermo Fisher Scientific). cDNA was denatured for 30 seconds at 98 °C, and amplified for 25 to 28 cycles of 5 seconds at 98 °C, 5 seconds at 62 °C and 15 seconds at 72 °C.

Semi-quantitative Analysis of Polyadenylated mRNA by a Coupled TVN-ePAT Assay

The protocol for analysis of polyadenylated HAdV-5 mRNA was based on (Janicke et al., 2012).

ePAT 5 µM universal primer A (**Table *2***) were annealed to 25 ng to 1 µg RNA for 5 minutes at 80 °C. Reactions were cooled to 37 °C, and 5 × SuperScript III Buffer (Invitrogen, Thermo Fisher Scientific), 5 mM DTT, 0,5 mM dNTP, and Klenow (-Exo, DNA polymerase I; New England Biolabs) were added. Samples were incubated for one hour at 37 °C, reactions inactivated for 5 minutes at 80 °C, and cooled to 55 °C. SuperScript III Reverse Transcriptase (Invitrogen, Thermo Fisher Scientific) was added directly to reactions incubated at 55 °C on the thermocycler. Samples were incubated at 55 °C for one hour, reactions inactivated for 5 minutes at 80 °C and cooled to 4 °C.

TVN-PAT 5 µM universal primer B (**Table *2***) were annealed to 25 ng to 1 µg RNA for 5 minutes at 80 °C. Reactions were cooled to 42 °C, and 5 × SuperScript III Buffer, 5 mM DTT, 0,5 mM dNTP, and SuperScript III Reverse Transcriptase were added. Samples were incubated for 15 minutes at 42 °C, 15 minutes at 48 °C, and 15 minutes at 55 °C. Reactions were inactivated for 5 minutes at 80 °C and cooled to 4 °C.

PCR cDNA was diluted 1 : 5 in sterile water prior to amplification by PCR applying universal primer C, primers targeting HAdV MTLU L2 – L5 transcripts, and the human control GAPDH primer A (Table 2). PCR reactions were carried out with the addition of 3 % DMSO according to the Phire Hot Start II DNA Polymerase protocol (Thermo Scientific, Thermo Fisher Scientific). cDNA was denatured for 30 seconds at 98 °C, and amplified for 22 to 28 cycles of 5 seconds at 98 °C, 5 seconds at 62 °C and 15 seconds at 72 °C. cDNA was analysed on agarose gels (1 × TBE, 2 % w/v UltraPure Agarose; Invitrogen, Thermo Fisher Scientific).
ePAT and TVN-PAT cDNA was analysed on agarose gels (1 × TBE, 2 % w/v agarose).

Table 2. Forward and reverse primer sequences

Primer	**Forward 5' – 3'**	**Reverse 5' – 3'**
TVN-PAT and ePAT assays		
Universal A		GCGAGCTCCGCGGCCGCGTTTTTTTTTTT
Universal B		GCGAGCTCCGCGGCCGCGTTTTTTTTTTT*TVN*
Universal C		GCGAGCTCCGCGGCCGCGT
L2	CGGCGG-TATCCTGCCCCTCCTTATT	
L3	GCAGCCACAGTGCGCAGATTAG-GAG	
L4	AGGGAGAGCTTGCCCGTAG	
L5	CCATTACACACTAAACGG-TACACAGGA	
GAPDH primer A	TCCTCACAGTTGCCATGTAG	
PCR and qPCR assays		
pV	CGAGGGACCTGAGCGAGTC	CCATAGATCTCCGGCGCGAT
pVI	CGAGGGACCTGAGCGAGTC	CTTGCCAGTTTCCCATGAACGG
L4-100K	AAACTAATGATGGCCGCAGTG	CGTCTGCCAGGTGTAGCATAG
Fiber	CGAGGGACCTGAGCGAGTC	GAGGACCGGTTTCCGTGTCA
18S rRNA	CCCCTCGATGCTCTTAGCTG	TCGTCTTCGAACCTCCGACT
GAPDH primer B	GGTTTACATGTTCCAATATGAT-TCCA	ATGGGATTTCCATTGATGACAAG
MALAT	GTCATAACCAGCCTGGCAGT	GCTTATTCCCCAATGGAGGT
tRNAlys	GCCCGGATAGCTCAGT	CGCCCAACGTGGGGCT

Metabolic Labelling of Newly Transcribed RNA by 4sU

Subsequent to 48 hours of siRNA treatment and 24 hours of infection, HAdV-5 transcription was analysed by metabolic labelling viral and human mRNAs with 4-thiouridine-5'-monophosphate (4sU), according to a protocol published by (Garibaldi et al., 2017). Cells were exposed to 150 µM 4sU for one hour. Simultaneous treatment of cells with the transcription inhibitor Actinomycin D (10 µg/mL) was used as a negative control. Cells were washed with 1 × PBS, pelleted for 30 seconds at 3.000 rpm, and RNA was isolated according to the manufacturer's protocol of TRI Reagent (Sigma-Aldrich, MilliporeSigma). RNA was reconstituted in 40 µL DEPC-treated water. Prior to the MTSEA-biotinylation procedure 5 % of total RNA were removed as input. For MSTEA-biotinylation 21 µg RNA were incubated with 10 × MTSEA labelling buffer (100 mM HEPES pH 7,5; 10 mM EDTA) and 5 µg MTSEA-Biotin-XX (Biotium) for 30 minutes at room temperature in darkness. RNA was cleaned twice by addition of equal volumes of chloroform, vortexing, centrifugation for 10 minutes at 12.000 × g and 4 °C and transferring the aqueous phase to new tubes. Equal volumes of 2-propanol, and 1:10 (v/v) of 5M NaCl were added to the aqueous phase. RNA was precipitated with the addition of 1 µL glycogen at -20 °C overnight to increase yields. RNA was pelleted for 20 minutes at 13.000 × g and 4 °C, washed with 75 % ethanol and reconstituted in 100 µL DEPC-treated water.

Streptavidin Magnetic Beads (New England Biolabs) were washed twice with washing/binding buffer (0,5 M NaCl; 20 mM Tris-HCl pH 7,5; 1 mM EDTA). RNA was captured by incubation with beads (2 µL/µg RNA) on a rotator for 30 minutes at room temperature. Beads were captured by a magnet and the supernatant removed (saved as reference). Beads were washed thrice with washing/binding buffer. MTSEA-biotinylated RNA was eluded with 25 mM DTT for 5 minutes at room temperature. Subsequently, RNA was concentrated using the RNA Clean & Concentrator – 25 (Zymo Research) according to the manufacturer's protocol. RNA was reverse transcribed into cDNA according to the SuperScript III Reverse Transcriptase protocol (Invitrogen, Thermo Fisher Scientific) and analysed by qPCR.

Surveillance of mRNA Stability via Selective Inhibition of RNA Polymerase II by DRB

Stability of viral transcripts was analysed after 24 hours of RNAi and subsequent 24 hours of HAdV-5 infection. Briefly, cells were exposed to 20 µg/mL 5,6-Dichloro-1-beta-Ribo-furanosyl Benzimidazole (DRB) for 0, 2, 4 and 6 hours. At indicated time points cell contents were fractionated according to the Cell Fractionation Kit protocol (Abcam). 16 % of initial cell suspensions were removed for western blot analysis. Samples allotted to RNA isolation were kept on ice until stored 1 : 3 in TRIzol LS (Invitrogen, Thermo Fisher Scientific) at -20 °C. RNA was reverse transcribed into cDNA according to the SuperScript III Reverse Transcriptase protocol (Thermo Fisher Scientific) and analysed by qPCR. Half-life calculations for viral pVI and L4-100K transcripts, as well as human control transcripts GAPDH, 18S rRNA and hPPARα were performed as a one phase decays in GraphPad Prism (version 9.2.0, GraphPad Software).

Quantitative Analysis of Viral Transcripts by qPCR

cDNA generated from total RNA, cytosolic or nuclear RNA was analysed in triplicate reactions with primers specific for HAdV-5 MLTU pV, pVI, L4-100K, fiber transcripts as well as ranscripts of housekeeping genes 18S and GAPDH (primer B) (Table *2*). The 5 × HOT FIREPol EvaGreen qPCR Mix Plus (ROX; Solis BioDyne) protocol was optimised through reduction of the reaction volume by 50 %, using between 5 to 10 ng cDNA, and primers at a final concentration of 125 nM. The qPCR protocol was followed as recommended by the manufacturer.

Western Blot Analysis

Equal volumes of whole cell lysates were separated on 8 % or 13 % SDS-PAGE in 1 × Running Buffer (25 mM Tris; 192 mM glycine; 1 % w/v SDS) for up to 2 hours at 80 to 110 V at room temperature. Proteins were transferred to 0,2 mm nitrocellulose membranes (Amersham) in 1 × Towbin Buffer (25 mM Tris, 192 mM glycine, pH 8.3, 10 % methanol) for 2 to 2,5 hours at 4 °C. Unspecific binding reactions were blocked with Intercept (PBS) Blocking Buffer (LI-COR) for 30 minutes at room temperature. Membranes were incubated with antibodies (primary 1 : 1.000, secondary 1 : 10.000) (Table 1) for up to 2 hours at room temperature, or at 4 °C overnight. Membranes were washed for 30 minutes in 1 × TBST (0,1%) prior to each incubation with antibodies. Indirect fluorescent signals of secondary antibodies were visualised by Odyssey CLx Imaging System (LI-COR).

Results

Depletion of PABPN1 from A549 cells negatively impacts HAdV-5 protein VI

The export of mRNAs from the nucleus via the nuclear pore complex (NPC) has been shown to be dependent on a multitude of different determinants as reviewed by Palazzo and Lee (2018). One such determinant is the polyadenylation of mRNA, partially controlled by the nuclear polyadenylate binding protein PABPN1. Another factor recently identified as a regulator of mRNA export through physical interaction with the nucleoporin GLE1 is the E3 ubiquitin-protein ligase MKRN2 (Wolf et al., 2020). To study the effects these proteins might have on viral mRNA export from the nucleus to the cytoplasm, RNA interference (RNAi) through small interfering RNAs (siRNA) was used to transiently deplete PABPN1 and MRKN2 proteins from HAdV-5 infected A549 cells.

Based on the notion that decreased mRNA levels in the cytoplasm will be reflected by a less efficient protein synthesis, various HAdV-5 proteins were analysed by western blotting. Proteins were extracted from A549 cells previously subjected to siRNA treatment, followed by infection with HAdV-5 for 20 or 40 hours. Virus-specific primary and host species-specific secondary antibodies were used to visualise proteins of interest. MKRN2 knockdown resulted in a general decrease of viral early (DBP) and late proteins (V, VI, VII) at 20 hours post infection (hpi), also affecting PABPN1 protein levels to a minor extent (Figure 3A). At 40 hpi transient MKRN2 depletion seemingly no longer impacted viral protein levels as visualised in **Figure *3***A. Interestingly, the effect that PABPN1 knockdown had on viral proteins was observed to be more selective. While proteins V, VII and L4-100K produced from the HAdV-5 major late transcription unit (MLTU), and the DNA binding protein (DBP/72K) expressed from the E2A transcription unit remained unaffected by the transient depletion of PABPN1 from cells, protein VI exhibited a distinct decrease at 20 hpi (**Figure *3***A and **Figure *3***B). At 40 hpi effects appeared to be less prominent (Figure 3), suggesting that the influence PABPN1 knockdown had on virus protein synthesis might be of a temporal nature. The occurrence of multiple bands of proteins DBP, V, VI (Figure 3A), VII (**Figure *4***) and L4-100K (**Figure *3***B) visualises the cleavage of the viral preproteins, generating multiple protein isoforms. The sample loading control actin remained unaffected in both siRNA treatments.

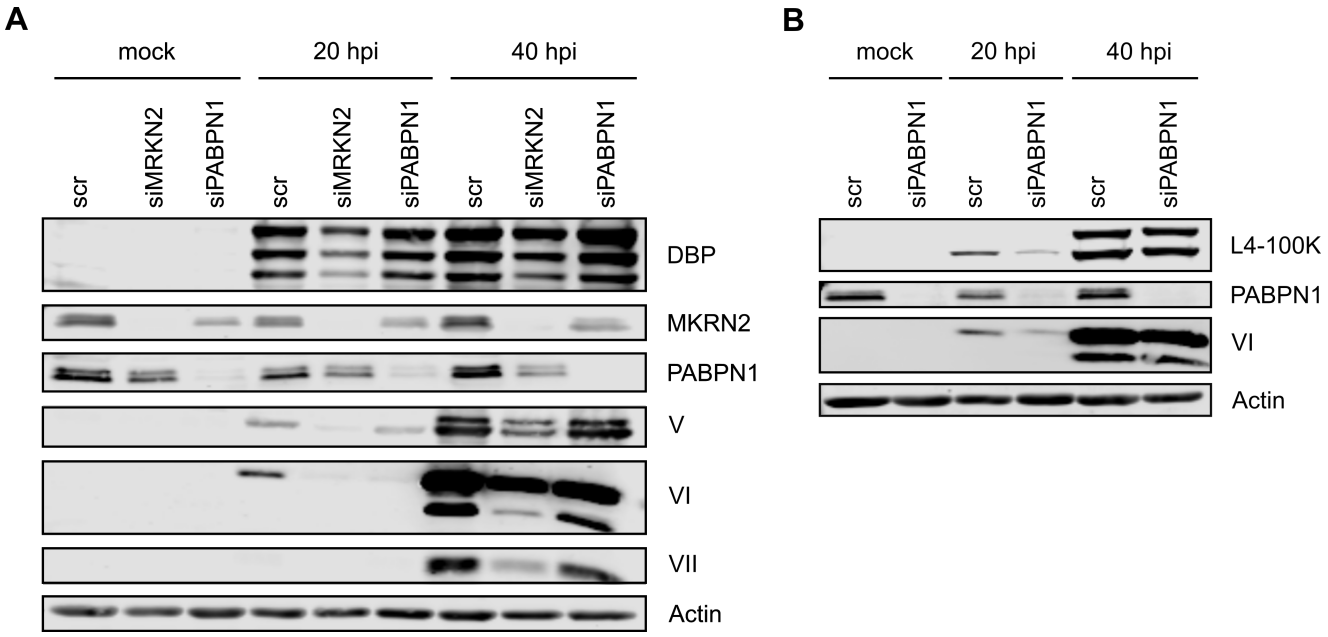

Figure 3. MKRN2 exhibits nonspecific effects on HAdV-5 proteins, whereas PABPN1 affects protein VI specifically. A549 cells were depleted of MRKN2 and PABPN1 through treatment with small interfering RNAs (siRNAs, 45 nM for 48 hours). Scramble (scr) as siRNA treatment control. Subsequently, cells were infected with HAdV-5 (MOI 10) and total protein was isolated at 20 and 40 hours post infection (hpi). Antibody-targeted proteins were visualised by western blotting. Cleavage of viral preproteins generates multiple protein isoforms, visible as distinct, multiple bands. **A.** MRKN2 knockdown negatively impacts virus MLTU proteins V, VI, VII and L4-100K, as well as E2A protein DBP at 20 hpi, whereas the effect subsided at 40 hpi. A, **B.** PABPN1 knockdown specifically impacts HAdV-5 protein VI, exhibiting the most prominent effect at 20 hpi, followed by a recovery of protein levels at 40 hpi. HAdV-5 proteins V, VII, L4-100K and DBP seemed to be unaffected by transient PABPN1 depletion at both time points. Actin levels are affected by MKRN2 depletion to minor levels but remain unaffected during PABPN1 knockdown.

PABPN1 knockdown does not affect E1A, suggesting a specificity for the MLTU protein VI

To further investigate the importance of PABPN1 during late phase HAdV-5 infection, a follow-up experiment was conducted using cleavage and polyadenylation specificity factor subunit 1 (CPSF1) as a positive control, and HAdV-5 proteins E1A and DBP as negative controls. It was assumed that transient depletion of CPSF1 would have a global negative impact on RNA processing and export, while data presented in **Figure *3*** suggested that transient depletion of PABPN1 specifically affected protein VI levels. To exclude possible upstream effects of PABPN1 on HAdV-5 replication, resulting in a general down-regulation of MLTU transcripts, the impact PABPN1 knockdown on E1A and DBP was studied. The HAdV-5 early protein E1A protein has been identified as an essential temporal regulator of HAdV-5 genes necessary for virus replication (reviewed by Gallimore and Turnell, 2001), while DBP has been established as a positive regulator for transcription of the HAdV-5 MLTU (Chang and Shenk, 1990).

To validate previously obtained data, A549 cells were treated with siRNA targeting CPSF1 and PABPN1, and subsequently infected with HAdV-5. Proteins from total lysates obtained at 20 and 40 hpi were targeted by virus-specific primary and host species-specific secondary antibodies. As anticipated, CPSF1 knockdown resulted in a strong negative impact on the prevalence of virus proteins at 20 hpi globally (**Figure *4***). Interestingly, this effect was reduced at 40 hpi. As depicted in **Figure *4***, transient PABPN1 depletion from A549 cells affected E1A and DBP protein levels to a negligible extent, whereas the effect on protein VI at 20 hpi was quite distinct. Furthermore, the previously observed PABPN1-

dependent effect on the MLTU L4-100K protein (Figure 3B) became visible at 20 hpi, though less prominent than the effect on protein VI. Corresponding to data depicted in Figure 3, effect of PABPN1 knockdown on viral proteins subsided at 40 hpi. Further corroborating previous observations, other proteins transcribed from the HAdV-5 MLTU, such as protein V and protein VII remained unaffected by PABPN1 knockdown. The lack of PABPN1 knockdown on the housekeeping proteins actin (**Figure *3***) and GAPDH (Figure 4) further suggests that the effect the transient depletion PABPN1 has on the HAdV-5 protein VI is of a selective nature.

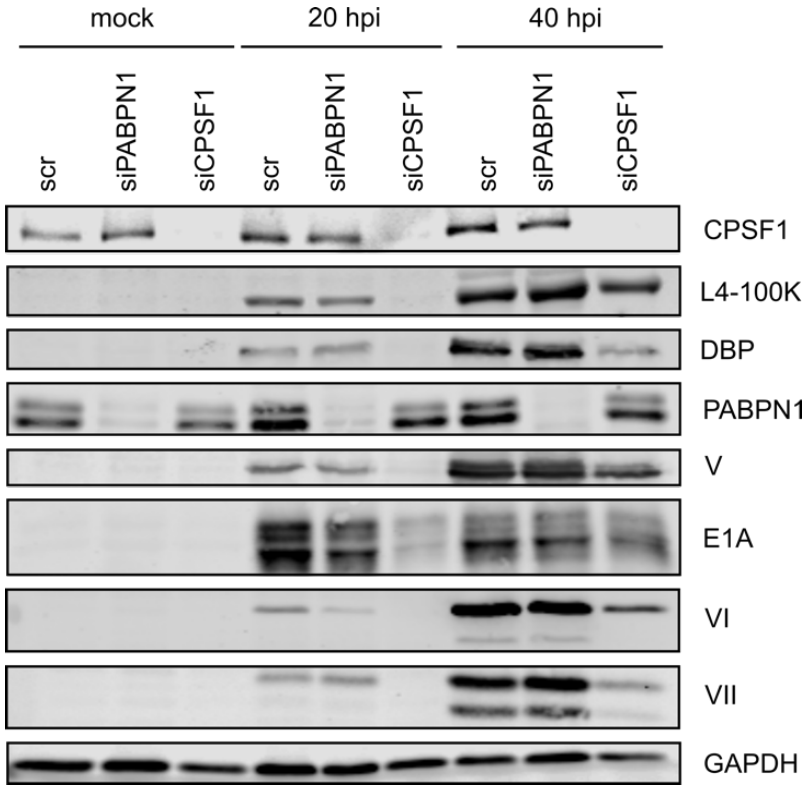

Figure 4. PABPN1 knockdown does not affect HAdV-5 MLTU proteins via upstream interference with E1A or DBP. Total protein extracts were obtained from A549 cells depleted of PAPBN1 or the cleavage and polyadenylation specificity factor subunit 1 (CPSF1) through RNA interference (RNAi, siRNA 45 nM for 48 hours), and subsequently infected with HAdV-5 (MOI 10). Scramble (scr) as RNAi treatment control. CPSF1 knockdown negatively impacts mRNA processing and export globally, reflected by a general decrease in HAdV-5 proteins at 20 hpi. At 40 hpi the effect was less prominent. Cellular proteins PABPN1 and GAPDH exhibit minor decrease in protein levels at both time points. PABPN1 knockdown elicits specific effects on proteins VI and L4-100K at 20 hpi, while remaining MLTU proteins V and VII, early protein E1A as well as DBP seemed to be unaffected by transient PABPN1 depletion. Multiple bands observed for L4-100K, E1A, VI and VII represent protein isoforms created by cleavage of viral preproteins. Loading control GAPDH is not affected by PABPN1 depletion.

PABPN1 localises from speckles to discrete circular structures during HAdV-5 infection

PABPN1 has been described to localise to nuclear speckles in an initial report by Krause et al. (1994). Speckles are nuclear compartments known to harbour aggregates of proteins involved in post-transcriptional pre-mRNA processing, such as small ribonucleoprotein particles (snRNPs), spliceosome subunits, and splicing factor SC35 (reviewed by Spector and Lamond, 2011). During HAdV-5 infection, transcription and splicing factors have been shown to be recruited to discrete nuclear compartments termed viral replication centres (Bosher et al., 1992; Bridge et al., 1995).

Based on these previous findings it was thus hypothesised that the spatial distribution of the endogenous PABPN1 protein would be altered in in HAdV-5 infected cells. To test this hypothesis, A549 cells were either mock infected or infected with HAdV-5. In order to study the effect of PABPN1 knockdown on viral protein localisation, a second set of A549 cells were further subjected to RNAi by siRNAs targeting PAPBN1. Proteins were targeted by anti-PABPN1 and anti-VII antibodies and visualised by fluorescently-tagged secondary antibodies through epifluorescence microscopy. As expected, PABPN1 localised to nuclear speckles in mock infected cells (Figure 5A, top row). However, in HAdV-5 infected cells PABPN1 was found to aggregate into circular structures located in proximity to the nuclear membrane at 24 hpi (Figure 5B, top row). Furthermore, characteristic swelling of the nucleus could be observed in virus infected cells. As depicted in Figure 5B, PABPN1 knockdown did not change the localisation of protein VII at 24 hpi, corroborating previously obtained data which indicates that the effect of transient PABPN1 depletion is specific to proteins VI and L4-100K (Figure 3A and B).

PABPN1 bimodal regulatory activity is dependent on individual MLTU polyadenylation sites

PABPN1 is implicated in the regulation of, *inter alia*, alternative cleavage and polyadenylation (APA) (de Klerk et al., 2012; Jenal et al., 2012; Simonelig, 2012), and RNA hyperadenylation and decay (Bresson and Conrad, 2013). Furthermore, previous data has shown that depletion of PAPBN1 from cells results in shortening of polyadenylate (polyA) tails of both nuclear and cytoplasmic RNAs (Benoit et al., 2005). The structure of the HAdV-5 major late transcription unit (MLTU) is defined by alternative polyadenylation sites giving rise to five mRNA families, and further subdivided into different mRNA species dependent on the use of alternative splice acceptor sites (Falck-Pedersen and Logan, 1989). Interestingly, recent findings by Donovan-Banfield et al. (2020) indicate that during the course of HAdV-5 infection viral transcripts exhibit shortening of polyA tails.

Thus, it was sought to determine the length of MLTU transcripts L2 to L5 in HAdV-5 infected A549 cells during late phase of infection. Total RNA was extracted from A549 cells that had previously been treated with siRNA targeting PABPN1 and CPSF1, and thereafter infected with HAdV-5 for 24 and 36 hours. To semi-quantitatively determine the polyadenylate tail length of viral RNAs, cDNA was generated according to a method proposed by Janicke et al. (2012). By coupling a TVN-PAT reaction with an extension polyadenylation test (ePAT), approximations on the actual length of virus RNA polyA tails could be made (**Figure *6***A). Briefly, PCR amplification of cDNA obtained from TVN-PAT reactions gives rise to amplicons reflecting an invariant polyA tail of 12 residues in length, whereas PCR products obtained from cDNA generated by ePAT reactions provide an overview on the distribution of polyA tails in a given sample. Comparison of both reactions enables approximation of the length of polyA tails of target RNAs (further clarification found in Figure 6A and Discussion).

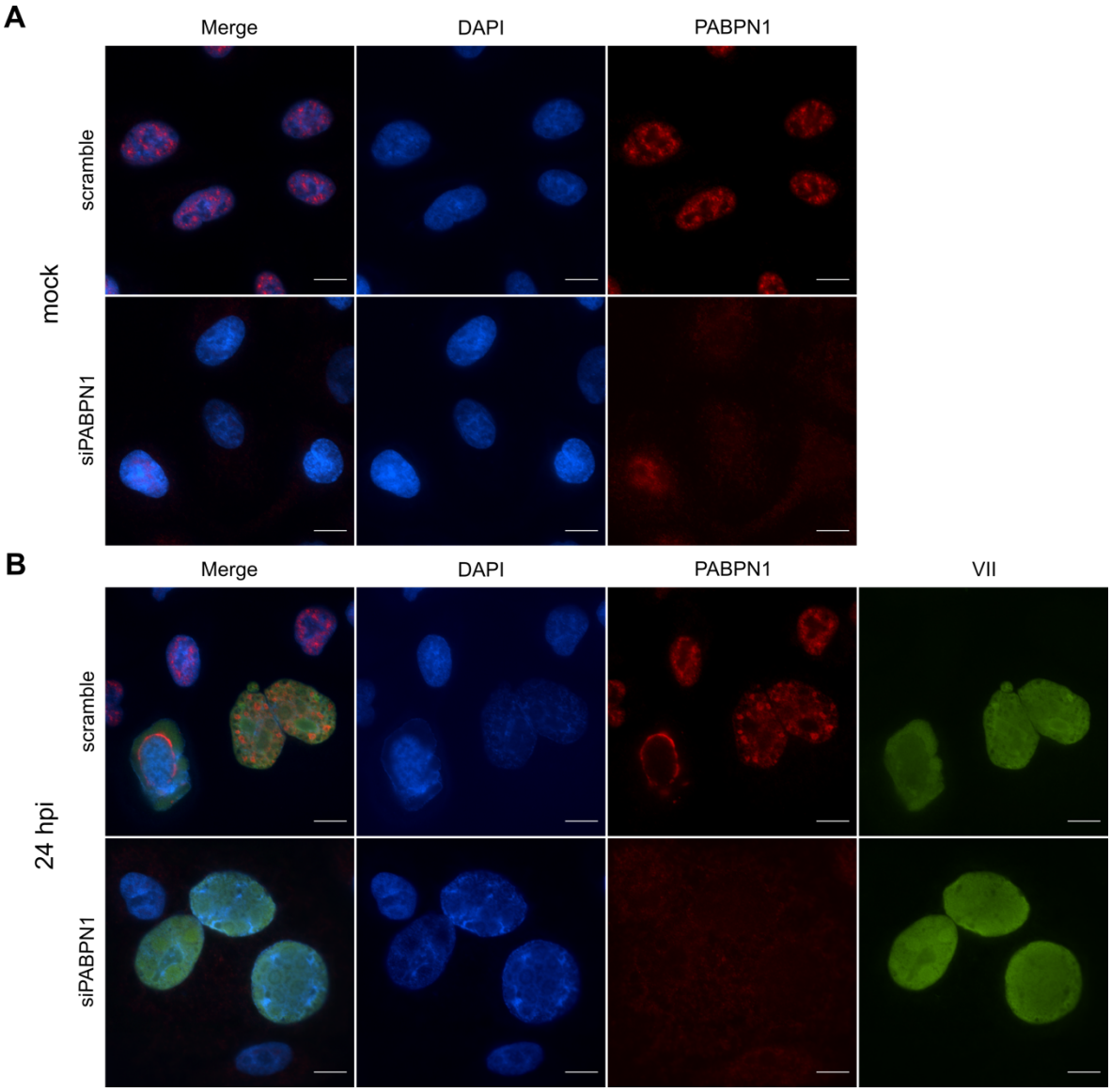

Figure 5. PABPN1 localises to circular structures in HAdV-5 infected cells. A549 cells were either mock infected or infected with HAdV-5 (MOI 10) and subjected to siRNA treatment targeting PABPN1 (45 nM for 48 hours). Scramble as RNAi treatment control. Cells were analysed by epifluorescence microscopy at 24 hpi. Proteins were targeted with anti-PABPN1 and anti-VII antibodies. DNA was stained with DAPI. **A.** In mock infected control cells (scramble), endogenous PABPN1 localises to distinct nuclear compartments termed nuclear speckles. **B.** During HAdV-5 infection PABPN1 localises to discrete circular structures located in proximity to the nuclear membrane. Depletion of PABPN1 from A549 cells through siRNA treatment did neither alter DNA structure nor localisation of the HAdV-5 protein VII. Scalebar 10 μm.

As can be observed in Figure 6B, transient depletion of CPSF1 from virus-infected cells results in an almost complete disappearance of polyA tails of MLTU transcripts L2 and L3 as visualised by both TVN and ePAT reactions at 24 hpi. Interestingly, this effect is reduced at 36 hpi, more strongly in L3 than L2, suggesting that the role of CPSF1 in viral pre-mRNA processing could be substituted by other cleavage and polyadenylation specificity factors. Unexpectedly, CPSF1 knockdown seems to have solely a negligible effect on HAdV-5 L4 transcripts at both time points. Thus, the increasing tail length of L3, and the

presence of polyA tails on L4 and L5 in absence CPSF1 at 36 hpi, indicates that PABPN1-dependent polyadenylation is still possible through functional compensation of CPSF1 knockdown by other CPSFs.

Strikingly, transient depletion of PABPN1 from HAdV-5 infected cells gave rise to varying polyA tails depending on the targeted RNA (Figure 6B). Indeed, while L2 transcripts exhibited a shortening in polyadenylate tails at both 24 and 36 hpi, L3 transcripts revealed an opposing trend through the elongation of polyadenylate tails at both 24 and 36 hpi. Similar to effects revealed in the case of CPSF1 knockdown, transient depletion of PABPN1 from infected cells apparently did not influence polyadenylation events on L4 transcripts at 24 or 36 hpi. Of further interest is the remarkable observation of a total lack of polyadenylation on L5 transcripts at 24 hpi. These findings would suggest that processing of MLTU L5 RNA, including polyadenylation, happens after 24 hpi, as made apparent by the distinct bands observed at 36 hpi. RNAs of the housekeeping gene GAPDH do not seem to be impacted by CPSF1 or PABPN1 knockdown. Band density analyses of TVN-PAT and ePAT cDNA products are depicted in Figure 6C, illustrating the CPSF1- or PABPN1-dependent shift of bands of HAdV-5 L2 to L5 transcripts, and GAPDH.

Transient PABPN1 depletion results in partial nuclear retention of HAdV-5 MLTU mRNAs

The importance of pre-mRNA processing such as splicing and polyadenylation, ensuring the export of mature mRNAs from the nucleus has been extensively reviewed (Palazzo and Lee, 2018). Further, based on the findings from studies by Paul and Montpetit (2016), and Muniz et al. (2015), highlighting the importance of pre-mRNA splicing for nuclear export, and the importance of PABPN1 in stimulating splicing events, respectively, the hypothesis that PABPN1 is a crucial factor in regulation of RNA export via the nuclear pore complex (NPC) was formulated. This notion was further strengthened by the effect visible on HAdV-5 proteins VI and L4-100K (Figure 3) in transiently PAPBN1-depleted cells, whose decrease at 20 hpi could thereby be readily explained.

Comparison of cytosolic to nuclear RNA and protein levels enabled examination of the effect PABPN1 knockdown had on export of HAdV-5 MLTU L2 to L5 RNAs from the nucleus, giving rise to proteins V, VI, L4-100K and fiber in the cytoplasm. A549 cells were transiently depleted of PABPN1 through siRNA treatment, followed by HAdV-5 infection. At 24 hpi RNA was isolated from the cytosol and nucleus through the consecutive lysis of plasmatic and nuclear membranes. Amplification of reverse transcribed cDNA by quantitative PCR (qPCR) revealed that RNA was partially accumulated in the nucleus in the absence of PABPN1. Despite this accumulation being a general trend, also affecting the housekeeping GAPDH RNA, the effect transient PABPN1-depletion has on the export of protein VI RNA is distinct (**Figure** 7A). Of further note is the partial accumulation of L4-100K RNA inside the nucleus of cells treated with siRNA targeting PABPN1. Despite PABPN1 knockdown resulting in partial nuclear accumulation of all viral RNAs as well as GAPDH, the absence of PABPN1 decreases protein VI levels selectively, whereas other proteins, including L4-100K do not seem to be affected (Figure 7B). These data corroborate data presented in **Figure *3*** and **Figure *4***.

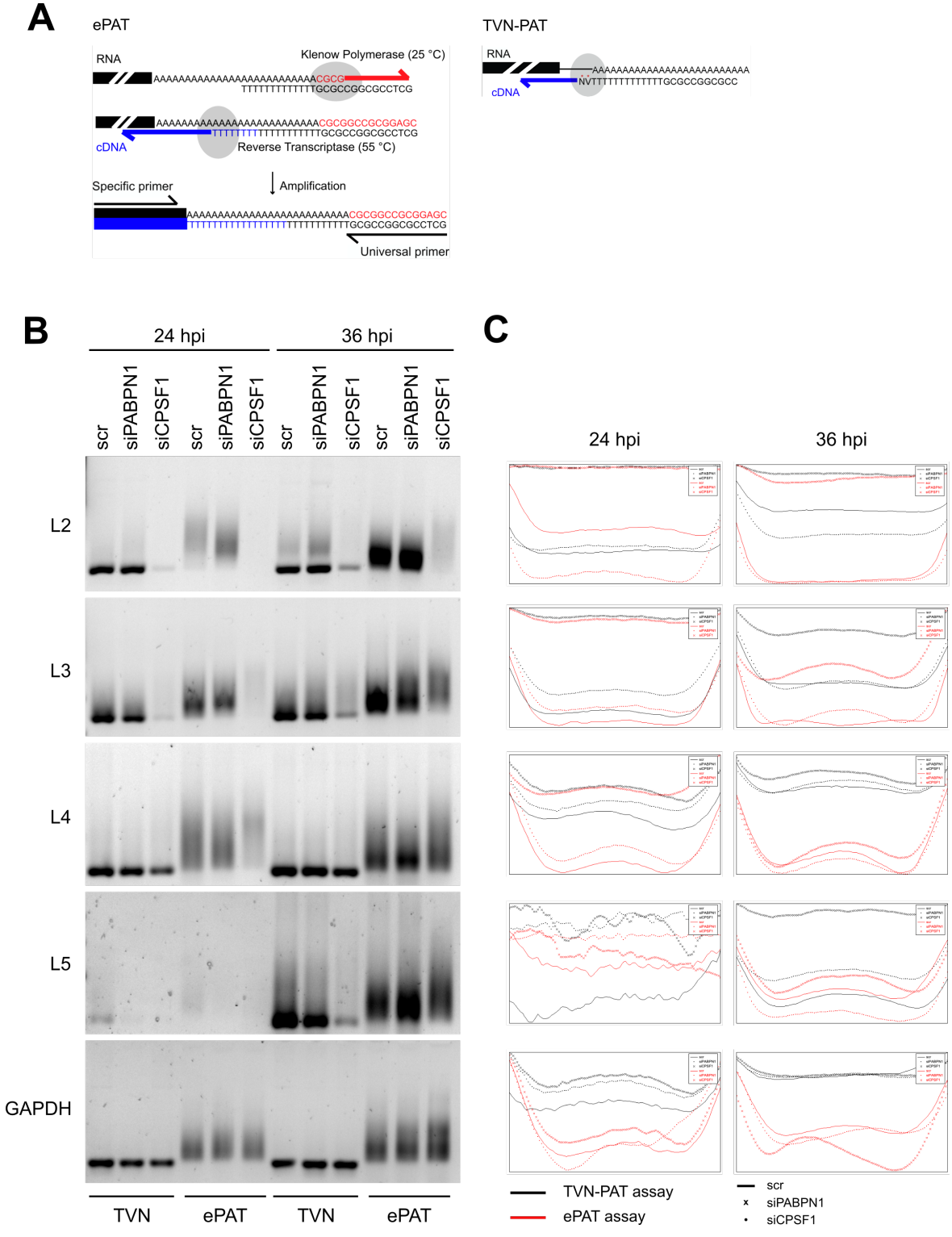

Figure 6. PABPN1-dependent polyadenylation of alternative HAdV-5 MLTU polyadenylation sites. A549 cells were treated with siRNA (45 nM, 48 hours) targeting CPSF1 or PABPN1, and infected with HAdV-5 (10). Scramble (scr) as siRNA treatment control. At 24 and 36 hours post infection (hpi) total RNA was isolated from cells. **A.** RNA was reverse transcribed into cDNA in either TVN-PAT or ePAT reactions. In ePAT reactions the Klenow polymerase extends RNA complementary to the DNA oligo(dT) template bound to polyadenylated stretches of target RNAs. Reverse transcription at 55 °C creates cDNA

that includes the artificially extended 3' UTR regions. PCR amplification of cDNA using a universal primer, binding to the extended 3' UTR, and a gene-specific primer produces differently sized amplicons, reflecting varying polyA tail lengths. In the TVN-PAT reaction the same DNA oligo(dT) template is used, however 3' modification by addition of V and N bases anchors the template to the first few adenosines of the polyA tail. Reverse transcription and amplification of cDNA with gene-specific primers results in amplicons of defined size, representing invariant polyA tails of 12 residues in length. Comparison between ePAT and TVN-PAT amplicons allows approximation of the polyA tail length. Panel A was adapted from Janicke et al. (2012) **B.** PABPN1 knockdown results in shortened polyA tails on HAdV-5 L2 RNA, while the polyA tails of L3 RNA become elongated. HAdV-5 L4 RNA remains unaffected by transient PABPN1 depletion. A striking observation can be done in case of the MLTU L5 RNA, whose polyadenylation seemingly takes place only after 24 hpi. The polyA tail of GAPDH RNAs exhibit negligible effects in transiently CPSF1 depleted cells. PCR products of TVN-PAT and ePAT reactions were separated on an ultra-resolution 2 % agarose gel. **C.** Band density analyses illustrate the shift resulting from varying polyadenylate tail lengths in a schematic way. Lane analysis was done with Fiji software (Schindelin et al, 2012).

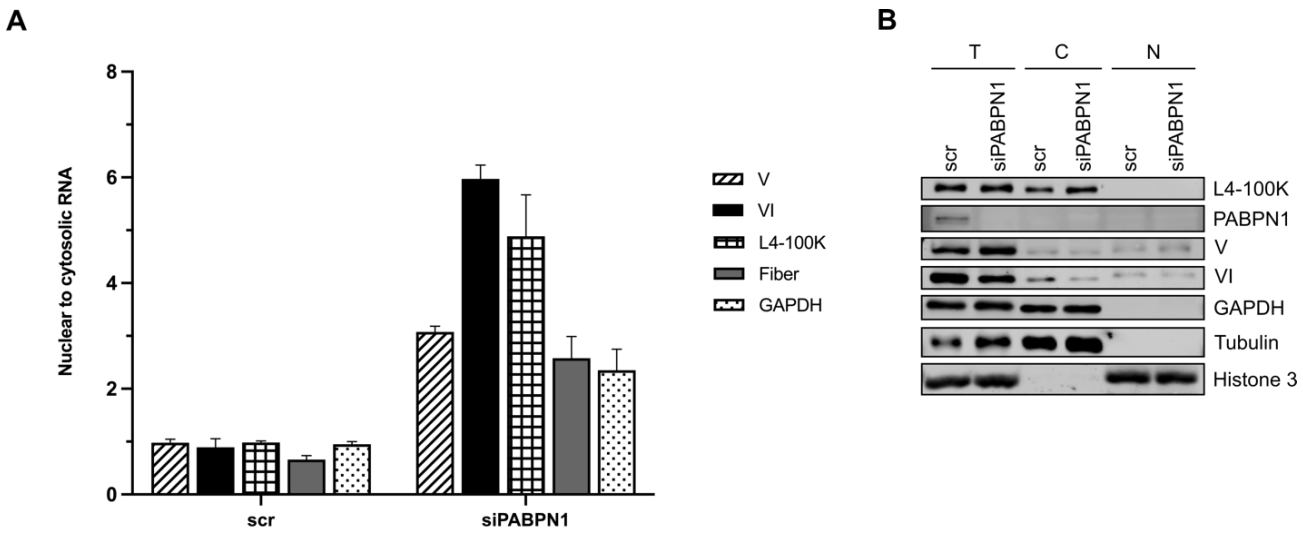

Figure 7. HAdV-5 MLTU RNAs are partially retained in the nucleus in the absence of PABPN1. PABPN1 was depleted from A549 cells through siRNA treatment (45 nM, 48 hours), and cells were infected with HAdV-5 (MOI 10) for 24 hours. Scramble (scr) as siRNA treatment control. Consecutive lysis of plasmatic and nuclear membranes allowed for isolation of RNA and proteins from cytosolic and nuclear fractions. **A.** Cytosolic and nuclear RNA isolated at 24 hpi was reverse transcribed into cDNA and amplified by qPCR. Data was normalised to total RNA and is presented as a ratio of nuclear to cytoplasmic RNA. PABPN1 knockdown caused a overall partial retention of HAdV-5 RNAs and the housekeeping GAPDH RNA. Transient depletion of PABPN1 from HAdV-5 infected cells had the strongest effect on protein pVI RNA, and revealed similar trends with regards to L4-100K RNA. **B.** Visualisation of HAdV-5 MLTU encoded proteins V, VI and L4-100K by western blotting. GAPDH acts as a loading control, whereas presence of the markers tubulin (cytoplasmic) and Histone 3 (nuclear) ensures a successful fractionation process. Comparison of total (T), cytosolic (C) and nuclear protein extracts allows observation of the effect nuclear RNA retention has on protein levels. PABPN1 knockdown specifically affects HAdV-5 protein VI, while remaining proteins V, L4-100K, GAPDH, tubulin and Histone 3 do exhibit a similar trend in the absence of PABPN1.

PABPN1 knockdown implies HAdV-5 RNA polyadenylation to be a nuclear event

Data published elsewhere (Afonina et al., 1998; Bhattacharjee and Bag, 2012) implies that transient depletion of PABPN1 is functionally compensated by a change in spatial distribution by shuttling polyadenylate binding proteins usually located in the cytoplasm into the nucleus. To establish whether polyadenylation of HAdV-5 MLTU RNAs was dependent on PABPN1 and thereby a strictly nuclear event, A459 cells were treated with PABPN1 siRNA and subsequently infected with HAdV-5 for 24 hours. RNA isolated from cytosolic and nuclear fractions was reverse transcribed into cDNA in TVN-PAT and ePAT reactions and amplified by PCR as previously described (Figure 6A).

As depicted in **Figure *8***A, the polyadenylation patterns of HAdV-5 MLTU L2 to L5 RNAs previously observed at 24 and 36 hpi (**Figure *6***B), are reflected in both cytosolic and nuclear RNAs, though to a less prominent extent than seen in total RNA isolates. L2 RNAs possess a shorter polyA tail in transiently PABPN1-depleted cells, whereas L3 polyA tails are slightly elongated in absence of PABPN1. Corroborating previously obtained data, and in line with findings published by Hector et al. (2002), L3 RNAs revealing elongated polyA tails are partially accumulated in the nucleus as can be seen in **Figure *7***A. Visualisation of cytoplasmic (tubulin) and nuclear markers (Histone 3) by western blotting (**Figure *7***B) validated successful isolation of cytosolic and nuclear fractions.

Discrepancies between the thickness of bands of cytosolic and nuclear extracts, reflecting the amount of cDNA amplified in PCR reactions, can be explained by the lower amounts of RNA obtained from nuclear than from cytosolic fractions. The overall faintness of bands observed in RNA isolated from siScr treated cells can be further reasoned to be a result of less efficient reactions during reverse transcription and PCR amplification due to worse RNA quality of that isolate. Thus, despite the semi-quantitative nature of TVN-PAT and ePAT assays, results depicted in **Figure *6***B and **Figure *8***A will solely be analysed in a quantitative manner. However, the effect on nuclear L2 and L3 RNA isolated from cells transiently depleted of PABPN1, remains distinctly visible, suggesting polyadenylation to be a nuclear PABPN1-dependent event. GAPDH polyA tails seemingly remained unaffected by PABPN1 knockdown in cytosolic and nuclear RNA isolates, as observed previously. Band density analyses of TVN-PAT and ePAT products are depicted in Figure 8B, illustrating the PABPN1-dependent shift of bands of HAdV-5 L2 and L3 transcripts.

HAdV-5 MLTU transcription is increased in PABPN1 depleted cells

Data presented in **Figure *7*** indicates PABPN1 to be a crucial factor regulating nuclear export of HAdV-5 RNAs, despite the extensive review on the role of RNA processing stating that polyadenylation is not essential for RNA export through the NPC (Palazzo and Lee, 2018). Further, opposing data has been put forth on the effect that PABPN1 depletion has on the general length and stability of RNA polyA tails (Bresson and Conrad, 2013; Meola et al., 2016). However, authors concur that PABPN1 is involved in negative regulation of nuclear RNA levels through exosomal decay. Thus, the proposed hypothesis that the partial nuclear accumulation of RNA resulted from nuclear retention of HAdV-5 RNAs in PABPN1-depleted cells, and was indeed not an artefact of a different effect altogether, needed validation. As the functional basis of the suggested PABPN1-dependent nuclear RNA retention remained elusive, it was sought to exclude the possibilities of (1) negative regulation of exosome-dependent decay, as well as (2) positive regulation of transcription, as has been observed for *MyoD* (Kim et al., 2001).

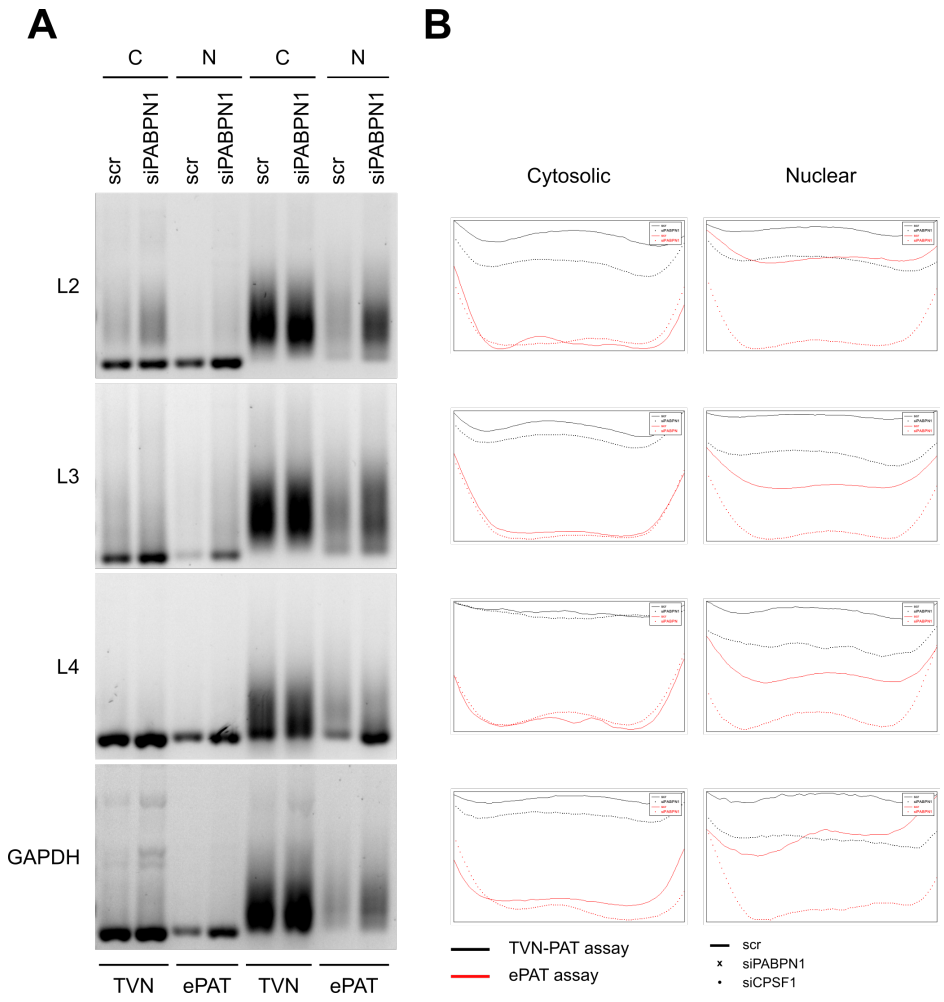

Figure 8. The length of polyadenylate tails of MLTU RNAs remains conserved in cytosolic and nuclear fractions, suggesting PABPN1-dependent polyadenylation in the nucleus. A. A549 cells were subjected to RNAi through siRNAs (45 nM for 48 hours) targeting PABPN1, and subsequently infected with HAdV-5 (MOI 10). Scramble (scr) as RNAi treatment control. At 24 hpi RNA was isolated from cytosolic (C) and nuclear (N) fractions and reverse transcribed into cDNA in TVN-PAT or ePAT reactions (Figure 6A). PABPN1 knockdown results in shortened polyA tails on HAdV-5 L2 cytosolic and nuclear RNA, while the polyA tails of L3 RNA become elongated. HAdV-5 L4 cytosolic and nuclear RNA remains unaffected by transient PABPN1 depletion. PCR products of TVN-PAT and ePAT reactions were separated on an ultra-resolution 2 % agarose gel. **B.** Band density analyses illustrate the PABPN1-dependent shift resulting from varying polyadenylate tail lengths in a schematic way. Lane analysis was done with Fiji software (Schindelin et al, 2012).

DRB (5,6-Dichloro-1-beta-Ribo-furanosyl Benzimidazole) is a classic inhibitor of transcription by RNA polymerase II (Baumli et al., 2010a; Sehgal et al., 1976). To establish the effect PABPN1 knockdown had on HAdV-5 RNA stability, A549 cells were treated with siRNA, followed by infection with HAdV-5 for 24 hours and exposure to DRB for 0, 2, 4 and 6 hours at late phase infection. Stabilisation of RNAs in absence of PABPN1 as described by Bresson et al. (2015) could not be reproduced as experimental data obtained remained inconclusive due to technical limitations (data not shown).

Next, it was sought to determine the effect that transient PABPN1 depletion had on the transcription rate of HAdV-5 RNAs. A549 cells were subjected to RNAi through siRNAs targeting PABPN1, and subsequently infected with HAdV-5 for 24 hours. Cells were supplied with 4sU (4-thiouridine), a naturally occurring uridine analogue for one hour, whereafter total RNA was isolated. Incorporation of 4sU metabolically labelled nascent RNAs, facilitating extraction from the pool of total RNAs through thiol-specific biotinylation (Rädle et al., 2013). Biotinylated 4sU RNA was reverse transcribed into cDNA and amplified by qPCR. Comparison of biotinylated RNA levels in PABPN1 depleted and control cells reveals that in the absence of PABPN1 viral transcription of HAdV-5 MLTU transcripts coding for protein VI and L4-100K was increased, implying PABPN1 to be a negative regulator of HAdV-5 transcription (Figure 9). GAPDH RNA levels remained unaffected in PABPN1 depleted cells.

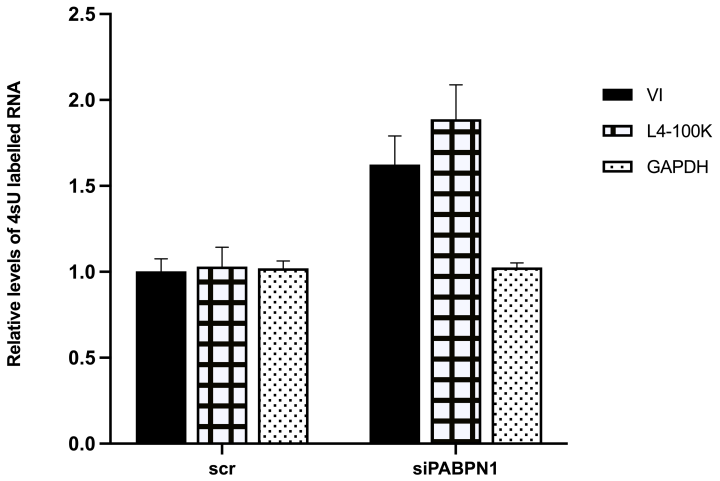

Figure 9. HAdV-5 transcription is negatively regulated by PABPN1. A549 cells were depleted of PABPN1 through siRNA treatment (45 nM, 48 hours), infected with HAdV-5 (MOI 10) for 24 hours. Scramble (scr) as control. Infected cells were exposed to 4sU for one hour. Thereby, nascent RNA was metabolically labelled. 4sU-specific biotinylation facilitated extraction of novel RNAs from a pool of total RNAs via streptavidin-coated beads selectively binding biotin. Tagged RNA was eluded, reverse transcribed and cDNA amplified with qPCR. Data was normalised to 18S rRNA and is depicted as a ratio of RNA levels obtained from untreated samples to RNA isolated from PABPN1 knockdown samples. HAdV-5 MLTU coding for either protein VI or L4-100K exhibited increased transcription in PABPN1 depleted cells. GAPDH remained unaffected by the siRNA treatment.

Discussion

Human adenoviruses (HAdVs) possess DNA genomes which comprise ten different transcription units. Similarly to other DNA viruses, HAdV transcription units are categorised into early, intermediate or temporal classes in relation to onset of DNA replication (Thomas and Mathews, 1980). Expression of HAdV late genes occurs from the major late transcription unit (MLTU), whose transcripts are assigned into five distinct families L1 to L5, dependent on the usage of alternative polyadenylation sites (Falck-Pedersen and Logan, 1989; Shaw and Ziff, 1980).

Polyadenylate binding proteins (PABPs) constitute a multi-functional class of regulatory proteins interacting with the 3' UTR of nascent RNAs. The functional versatility of the nuclear polyA-binding protein PABPN1 is made apparent by its regulation of alternative cleavage and polyadenylation (APA) (de Klerk et al., 2012; Jenal et al., 2012; Simonelig, 2012), and of stoichiometry-dependent RNA hyperadenylation and decay (Bresson and Conrad, 2013). Based on findings presented in this study, a novel role for PABPN1 in nuclear export of HAdV-5 mRNA, independent of its function as a regulator of polyA tail length is suggested.

The visually most stimulating evidence for the relevance of PABPN1 in HAdV-5 infections is highlighted by the epi-immunofluorescent imaging of PABPN1 localisation to circular structures in HAdV-infected cells, as in comparison to nuclear speckles in mock-infected cells (**Figure *5***). It was presumed that these circular structures are HAdV-5 virus replication centres (VRCs) as similar structures have been described previously (Charman and Weitzman, 2020 (for review); Genoveso et al., 2020; Hidalgo and Gonzalez, 2019; Reyes et al., 2017). However, further high-resolution imaging has to be done using antibodies against the HAdV-5 DNA-binding protein DBP (72K), a marker for VRCs (Chang and Shenk, 1990; Kruijer et al., 1983), to validate that PABPN1 is indeed localising to the VRCs, and not to the nuclear pore complex for example, which could exhibit similar phenotypes as observed. Furthermore, it would be of interest to elucidate the nature of the translucent halos that have become visible in the nucleoplasm of infected cells (DAPI staining), and to exclude them as possible VRCs.

It does not come as a surprise that PABPN1 would be recruited to VRCs. The primarily cytoplasmic PABPC1 has been described as a "common target" in virus infections. Some viruses exert negative regulatory effects on PABPC1. Such is the case for picornaviruses which elicit cleavage of PABPC1, whereby the interaction between PAPBC1 and eIF4G during translation initiation is prevented, inhibiting efficient host protein synthesis. Other viruses are dependent on PAPBC1 activity. Human cytomegalovirus (HCMV) recruits PABPC1 to the eIF4F complex, increasing the efficiency of translation initiation, while Dengue virus and vaccinia virus promote virus translation by recruiting PABPC1 to the viral RNA 3' UTRs and virus replication centres, respectively (reviewed by Smith and Gray, 2010). Still, virus-dependent recruitment of PABPN1 to VRCs has not yet been described.

The abundance of cellular proteins is controlled by a multitude of events, such as transcription rate, nuclear export of mRNAs, cytoplasmic transcript decay, translational regulation, availability of ribosomes and formation of polysomes during translation (Katahira, 2012 for review; Riba et al., 2019; Sonenberg and Hinnebusch, 2009). Initial analysis of protein expression in MKRN2-, PABPN1- or CPSF1- depleted cells indicates that all these three RNA-binding proteins (RBPs) exhibit a negative impact on HAdV-5 protein synthesis on a post-transcriptional level. While MKRN2 and CPSF1 knockdown elicited a global effect on virus proteins at 20 hpi (Figure 3, 4), absence of PABPN1 revealed a distinct effect on HAdV-5 protein VI, and to minor extent on protein L4-100K. These negative impacts on protein levels subsided at 40 hpi. Upstream effects of transient PABPN1 depletion on HAdV-5 transcription were excluded as pro-

tein levels of E1A, essential in transcriptional stimulation (Lillie et al., 1987), and DBP (72K), involved in DNA replication (Kruijer et al., 1983) remained unchanged (**Figure *4***). Thereby, the DNA replication-dependent transcription of late genes by selective activity of APA sites (Thomas and Mathews, 1980) was shown not to be compromised.

Previous studies have described the human MKRN2, and the yeast PABP Nab2 as regulators of nuclear RNA export through physical interaction with subunits of the nuclear pore complex (NPC) (Adams and Wente, 2020; Hector et al., 2002; Schmid et al., 2015; Wolf et al., 2020). CPSF1 is a subunit of the cleavage and polyadenylation complex, ensuring processing of pre-mRNA prior to polyadenylation and nuclear export (Davis et al., 2019; Neve et al., 2017). Thus, decreased protein synthesis in absence of MKRN2 and CPSF1 does not surprise. Pab2 is a homolog of PABPN1 exclusively found in *Schizosaccharomyces pombe*, whereas a *Saccharomyces cerevisiae* orthologue to PABPN1 has not yet been described (Perreault et al., 2007). Despite *S. cerevisiae* Nab2 being a homologue to the human ZC3H14 and not PABPN1, the interaction between Nab2, Pab1p and CPF (homologous to human PABPC1 and CPSF, respectively), and the human PABPN1 and CPSF1 (Turtola et al., 2021), exhibit orthologous functionality affecting RNA processing and ultimately regulating nuclear RNA export.

Importantly, as eloquently stated in a review by Liu et al. (2016), the spatial and temporal variations of RNAs as well as the local availability of the translation machinery can strongly influence protein synthesis. Nevertheless, protein levels do not necessarily proportionally relate to transcript abundance (Donovan-Banfield et al., 2020), which was highlighted by the apparent dissonance between the abundance of protein VI transcripts and cytoplasmic protein VI levels. The distinct decrease of protein VI was not reflected by a decrease of cytoplasmic protein VI-encoding RNA (data not shown). Considering previously published data (Afonina et al., 1998; Calado et al., 2000), describing PABPN1 to shuttle between the nucleus and the cytoplasm, these findings indicate a particular role for PABPN1 in the cytoplasm. The cytoplasmic counterpart of PABPN1, PABPC1 is needed for efficient translation initiation (reviewed by Smith and Gray, 2010), thus, a similar role for PABPN1 in HAdV-5 infections, exclusive to certain late virus proteins, such as protein VI (and L4-100K) could be suggested. However, in absence of clear evidence for a cytoplasmic role of PABPN1 in HAdV-5 infection, this study instead focussed on the investigation of RNA processing and stability.

The influence of PABPN1 on HAdV-5 transcripts, more specifically RNAs transcribed from the MLTU, was indirectly visualised by generation of cDNA according to a PCR protocol designed to particularly reveal the length of the polyA tail of RNAs (Beilharz and Preiss, 2009; Janicke et al., 2012). Interestingly, varying levels of processing and aberrant polyA tail lengths were observed on different MLTU RNAs in PABPN1-depleted cells in a spatiotemporal manner. L2 and L5 RNAs revealed polyA tail shortening, while L3 RNAs exhibited a particular elongation of polyA tails. L4 RNAs remained unaffected during PAPBN1 knockdown, whereas L5 RNAs polyA tails were observed solely at 36 hpi (**Figure *6***). This remarkable effect of a lack of polyadenylation on L5 transcripts at 24 hpi suggests that processing and polyadenylation of MLTU L5 indeed happens later than 24 hpi, as the absence of bands at 24 hpi due to technical limitations can be excluded.

These data corroborate previous reports of the general necessity of DNA replication for induction of efficient MLTU transcription, with the exception of the MLTU RNAs L1, and unexpectedly L4, that have been described to already be present during early to intermediate phases of infection. Nevertheless, efficient transcription of L2, L3 and L5 RNAs through the selection of respective APA sites appears to require the synthesis of specific regulatory factors not present during early to intermediate infection stages (Larsson et al., 1992). Further validation of these findings was achieved through a follow-up experiment visualising polyA tails of cytosolic and nuclear fractions of HAdV-5 MLTU RNAs. Polyadenylation

trends previously observed in the absence of PABPN1 (Figure 8) were once more present on cytosolic and nuclear L2 and L3 RNAs. The similarity between cytosolic and nuclear polyA tails strengthens the hypothesis of nuclear, PABPN1-dependent polyadenylation of HAdV-5 RNAs. Interestingly, an unexpected cytoplasmic activity of PABPN1, resulting in the shortening of certain RNAs during *Drosophila* early development has been described (Benoit et al., 2005). Nonetheless, in a scenario of PABPN1-independent cytoplasmic polyadenylation changes in polyA tail lengths of cytosolic RNAs through the activity of cytoplasmic PABPs such as PABPC1 would be expected.

Previous reports by de Klerk et al. (2012) and Jenal et al. (2012) have identified PABPN1 as a negative regulator of alternative polyadenylation, and that cellular 3' UTRs experienced universal shortening to lengths between 50 to 150 nucleotides (Bresson and Conrad, 2013) through the enhanced selection of proximal polyA sites in absence of PABPN1. During the course of HAdV-5 infection, virus transcripts exhibit general shortening as recently described by Donovan-Banfield et al. (2020), independent of PABPN1 availability. However, these findings could not be validated through the method employed in this study which comprises the combination of TVN-PAT and ePAT reactions. During the ePAT reaction a universal DNA primer comprising oligo(dT) stretches anneals to extended adenylate stretches of RNA. Thereby, the 3' UTR of RNAs can be extended, and functions as a binding platform for a universal primer, specific to the extended 3' UTR region, that is used in subsequent PCR amplification of cDNA. The same primer is applied during a separate TVN-PAT reaction, with the exception of harbouring a modified 3' end. Addition of the two variable bases V (A, G, or C) and N (any base) anchors the primer to a specific site at the 3' UTR, whereby the length of the TVN-PAT product becomes invariable (12 nucleotides), irrespective of the actual polyA tail length of targeted RNAs. Smeared bands visible in **Figure *6***, 8 thereby visualise the variation of polyA tail lengths of RNAs within the sample, and allow the estimation of the polyA tail by comparing the bands to invariant-length bands of the TVN-PAT reaction. However, direct measurement of polyA tail length cannot be achieved through this method, highlighting the need of a northern blot analysis or Nanopore high-throughput sequencing of HAdV-5 MLTU RNAs in future studies.

Comparison of cytosolic to nuclear HAdV-5 RNAs indicated that in the absence of PABPN1 RNAs exhibited partial nuclear retention that could not be observed when PABPN1 was present (**Figure *7***). MLTU encoded proteins VI (L3) and protein L4-100K (L4) were affected most, an effect that was visible on a protein level solely in the case of protein VI (Figure 3, 4). Similar nuclear retention during PABPN1 knockdown was previously described in *in vitro* cultivated murine muscle cells that exhibited shortening of RNA polyA tails and impaired export of transcripts into the cytoplasm (Apponi et al., 2010). Yet, in the absence of solid data on the polyA tail length of HAdV-5 MLTU transcripts, explainable by the comparatively low resolution of TVN-PAT and ePAT reactions (in contrast to RNA sequencing), the actual importance of the presence of either the polyA tail or PAPBN1, or a combination of both factors (Fuke and Ohno, 2008) for nuclear export cannot be determined. Therefore, conclusive data verifying PABPN1 involvement in nuclear export independent of its role in polyadenylation have yet to be gathered.

Observations concerning nuclear export or retention of RNAs are solely possible when cellular contents are separated, allowing isolation of proteins and RNA from the cytosol and nucleoplasm. This separation, as aforementioned and described in *Materials and Methods,* can be achieved employing various strategies. Methods evaluated in this study comprise commercially available kits as well as fractionation protocols found in literature. However, despite all methods providing protein fractions of satisfactory purity, solely commercially available kits ensured RNA fractions without contamination when protocols were followed as suggested by the manufacturer. Downscaling of experimental setups was not successful and resulted in contaminated fractions (data not shown).

Nuclear export of RNAs is an intricate process whose complete functional evaluation with regards to the general export of HAdV-5 transcripts lies not within the scope of this study. As extensively reviewed by Palazzo and Lee (2018) there are several determinants active on the RNA level regulating the nuclear export of transcripts. Further regulation is exerted by the NPC and associated factors, some of which evidently become targets of manipulation during virus infections (Bonnet and Palancade, 2014). To circumvent these factors limiting this study, the focus was instead centred on viral RNA stability and HAdV-5 transcriptional activity. The first attempt at a possible explanation for the enrichment of HAdV-5 MLTU RNAs within the nucleus during PABPN1 knockdown, was to define whether viral RNAs would be more stable in PABPN1-depleted cells. Thereby, PABPN1-dependent hyperadenylation and exosome-mediated decay (Bresson and Conrad, 2013) were excluded, and transcription was inhibited by the chemical DRB (5,6-dichlorobenzimidazone-1-b-D-ribofuranoside), disrupting P-TEFb dependent stimulation of RNA polymerase II (Baumli et al., 2010b; Bresson et al., 2015; Sehgal et al., 1979) (data not shown). However, preliminary data obtained remains inconclusive and requires further experimental validation.

In a second attempt to identify a possible reason for the accumulation of MLTU RNAs within the nucleus of PABPN1-depleted cells, the transcriptional activity of HAdV-5 was surveilled by metabolic labelling of nascent transcripts with the naturally occurring uridine analogue 4sU (4-thiouridine) (Rädle et al., 2013). Interestingly, in the absence of PABPN1 more MLTU RNA coding for proteins VI and L4-100K was transcribed (Figure 9), suggesting PABPN1 to function a negative regulator of HAdV-5 infection. These data oppose the logical presumption that an increase of proteins VI and L4-100K should be observed. Indeed, as aforementioned, PABPN1 knockdown decreased levels of protein VI specifically (Figure *3*, 4).

In conclusion, this study has revealed that HAdV-5 MLTU transcripts are polyadenylated by PABPN1 in a temporally-regulated manner, and specific to the APA site used. Implications these modifications have were assumed to relate to enhanced virus RNA stability or export from the nucleus. However, neither increased stability nor elevated protein production were observed during PABPN1 knockdown. Instead, an increase in transcription of HAdV-5 MLTU RNA was revealed, which unexpectedly did not translate to elevated translational activity. Yet, the partial nuclear accumulation of virus RNA, the cytoplasmic presence of the nuclear marker MALAT1 (Nakagawa et al., 2012; Tripathi et al., 2010), and the nuclear presence of the cytoplasmic marker $tRNA^{lys}$ (Rubio and Hopper, 2011; Turunen et al., 2019) in PABPN1-depleted but not control cells (data not shown) suggests PABPN1 to be involved in nuclear export in a polyadenylation-independent manner. Thus, the precise implications of aberrant PABPN1-dependent MLTU polyadenylation, and the role of PABPN1 in nuclear RNA export remain to be unveiled.

There are certain factors that can be assumed as limiting in this study. Experiments have to be repeated in cells overexpressing PABPN1, and in knock-out cells where PABPN1 depletion can be rescued by transfection. This will verify that effects observed in this study are truly caused by PABPN1 and not unexpected artifacts generated by PABPN1 interaction partners. Moreover, normalisation methods applied during data analysis should be optimised further, and data obtained in decay and metabolic labelling experiments validated though repetition.

Acknowledgements

I would like to especially thank Dr. Tanel Punga for providing me with the opportunity to switch projects last second when it was necessary, and to have welcomed me back to the research group with open arms. I highly appreciated the stimulating working environment, the provided guidance, and the independence that I was given during my project. Thus, I want to express my gratitude for the trust that was put in me.

Further, I would like to thank Dr. Ravi Inturi for lending a helping hand, mind, and equipment when needed. Last but not least, I want to express my warm thanks to the colleagues of Göran Akusjärvi's research group, and the office for making work such an enjoyable time.

References

Adams, R.L., Wente, S.R., 2020. Dbp5 associates with RNA-bound Mex67 and Nab2 and its localization at the nuclear pore complex is sufficient for mRNP export and cell viability. PLoS Genet 16, e1009033. https://doi.org/10.1371/journal.pgen.1009033

Afonina, E., Stauber, R., Pavlakis, G.N., 1998. The Human Poly(A)-binding Protein 1 Shuttles between the Nucleus and the Cytoplasm. Journal of Biological Chemistry 273, 13015–13021. https://doi.org/10.1074/jbc.273.21.13015

Apponi, L.H., Leung, S.W., Williams, K.R., Valentini, S.R., Corbett, A.H., Pavlath, G.K., 2010. Loss of nuclear poly(A)-binding protein 1 causes defects in myogenesis and mRNA biogenesis. Human Molecular Genetics 19, 1058–1065. https://doi.org/10.1093/hmg/ddp569

Baumli, S., Endicott, J.A., Johnson, L.N., 2010a. Halogen Bonds Form the Basis for Selective P-TEFb Inhibition by DRB. Chemistry & Biology 17, 931–936. https://doi.org/10.1016/j.chembiol.2010.07.012

Baumli, S., Endicott, J.A., Johnson, L.N., 2010b. Halogen Bonds Form the Basis for Selective P-TEFb Inhibition by DRB. Chemistry & Biology 17, 931–936. https://doi.org/10.1016/j.chembiol.2010.07.012

Bear, D.G., Fomproix, N., Soop, T., Björkroth, B., Masich, S., Daneholt, B., 2003. Nuclear poly(A)-binding protein PABPN1 is associated with RNA polymerase II during transcription and accompanies the released transcript to the nuclear pore. Experimental Cell Research 286, 332–344. https://doi.org/10.1016/S0014-4827(03)00123-X

Beaulieu, Y.B., Kleinman, C.L., Landry-Voyer, A.-M., Majewski, J., Bachand, F., 2012. Polyadenylation-Dependent Control of Long Noncoding RNA Expression by the Poly(A)-Binding Protein Nuclear 1. PLoS Genet 8, e1003078. https://doi.org/10.1371/journal.pgen.1003078

Beilharz, T.H., Preiss, T., 2009. Transcriptome-wide measurement of mRNA polyadenylation state. Methods 48, 294–300. https://doi.org/10.1016/j.ymeth.2009.02.003

Benoit, B., Mitou, G., Chartier, A., Temme, C., Zaessinger, S., Wahle, E., Busseau, I., Simonelig, M., 2005. An Essential Cytoplasmic Function for the Nuclear Poly(A) Binding Protein, PABP2, in Poly(A) Tail Length Control and Early Development in Drosophila. Developmental Cell 9, 511–522. https://doi.org/10.1016/j.devcel.2005.09.002

Bhattacharjee, R.B., Bag, J., 2012. Depletion of Nuclear Poly(A) Binding Protein PABPN1 Produces a Compensatory Response by Cytoplasmic PABP4 and PABP5 in Cultured Human Cells. PLoS ONE 7, e53036. https://doi.org/10.1371/journal.pone.0053036

Bonnet, A., Palancade, B., 2014. Regulation of mRNA Trafficking by Nuclear Pore Complexes. Genes 5, 767–791. https://doi.org/10.3390/genes5030767

Bosher, J., Dawson, A., Hay, R.T., 1992. Nuclear factor I is specifically targeted to discrete subnuclear sites in adenovirus type 2-infected cells. J Virol 66, 3140–3150. https://doi.org/10.1128/jvi.66.5.3140-3150.1992

Bresson, S.M., Conrad, N.K., 2013. The Human Nuclear Poly(A)-Binding Protein Promotes RNA Hyperadenylation and Decay. PLoS Genet 9, e1003893. https://doi.org/10.1371/journal.pgen.1003893

Bresson, S.M., Hunter, O.V., Hunter, A.C., Conrad, N.K., 2015. Canonical Poly(A) Polymerase Activity Promotes the Decay of a Wide Variety of Mammalian Nuclear RNAs. PLoS Genet 11, e1005610. https://doi.org/10.1371/journal.pgen.1005610

Bridge, E., Xia, D.X., Carmo-Fonseca, M., Cardinali, B., Lamond, A.I., Pettersson, U., 1995. Dynamic organization of splicing factors in adenovirus-infected cells. J Virol 69, 281–290. https://doi.org/10.1128/jvi.69.1.281-290.1995

Calado, A., Kutay, U., Kühn, U., Wahle, E., Carmo-Fonseca, M., 2000. Deciphering the cellular pathway for transport of poly(A)-binding protein II. RNA 6, 245–256. https://doi.org/10.1017/S1355838200991908

Chang, L.-S., Shenk, T., 1990. The adenovirus DNA-binding protein stimulates the rate of transcription directed by adenovirus and adeno-associated virus promoters. J Virol 64, 2103–2109. https://doi.org/10.1128/jvi.64.5.2103-2109.1990

Charman, M., Weitzman, M.D., 2020. Replication Compartments of DNA Viruses in the Nucleus: Location, Location, Location. Viruses 12, 151. https://doi.org/10.3390/v12020151

Chen, Z., 1999. Influenza A virus NS1 protein targets poly(A)-binding protein II of the cellular 3'-end processing machinery. The EMBO Journal 18, 2273–2283. https://doi.org/10.1093/emboj/18.8.2273

Chow, L.T., Broker, T.R., 1978. The Spliced Structures of Adenovirus 2 Fiber Message and the Other Late mRNA. Cell 15.

Davis, M.R., Delaleau, M., Borden, K.L.B., 2019. Nuclear eIF4E Stimulates 3′-End Cleavage of Target RNAs. Cell Reports 27, 1397-1408.e4. https://doi.org/10.1016/j.celrep.2019.04.008

de Klerk, E., Venema, A., Anvar, S.Y., Goeman, J.J., Hu, O., Trollet, C., Dickson, G., den Dunnen, J.T., van der Maarel, S.M., Raz, V., 't Hoen, P.A.C., 2012. Poly(A) binding protein nuclear 1 levels affect alternative polyadenylation. Nucleic Acids Research 40, 9089–9101. https://doi.org/10.1093/nar/gks655

Denney, L., Branchett, W., Gregory, L.G., Oliver, R.A., Lloyd, C.M., 2018. Epithelial-derived TGF-β1 acts as a pro-viral factor in the lung during influenza A infection. Mucosal Immunol 11, 523–535. https://doi.org/10.1038/mi.2017.77

Dickinson, M., Kliszczak, A.E., Giannoulatou, E., Peppa, D., Pellegrino, P., Williams, I., Drakesmith, H., Borrow, P., 2020. Dynamics of Transforming Growth Factor (TGF)-β Superfamily Cytokine Induction During HIV-1 Infection Are Distinct From Other Innate Cytokines. Front. Immunol. 11, 596841. https://doi.org/10.3389/fimmu.2020.596841

Donovan-Banfield, I., Turnell, A.S., Hiscox, J.A., Leppard, K.N., Matthews, D.A., 2020. Deep splicing plasticity of the human adenovirus type 5 transcriptome drives virus evolution. Commun Biol 3, 124. https://doi.org/10.1038/s42003-020-0849-9

Elkon, R., Ugalde, A.P., Agami, R., 2013. Alternative cleavage and polyadenylation: extent, regulation and function. Nat Rev Genet 14, 496–506. https://doi.org/10.1038/nrg3482

Falck-Pedersen, E., Logan, J., 1989. Regulation of poly(A) site selection in adenovirus. J Virol 63, 532–541. https://doi.org/10.1128/jvi.63.2.532-541.1989

Fessler, S.P., Young, C.S.H., 1998. Control of Adenovirus Early Gene Expression during the Late Phase of Infection. J Virol 72, 4049–4056. https://doi.org/10.1128/JVI.72.5.4049-4056.1998

Fuke, H., Ohno, M., 2008. Role of poly (A) tail as an identity element for mRNA nuclear export. Nucleic Acids Research 36, 1037–1049. https://doi.org/10.1093/nar/gkm1120

Gallimore, P.H., Turnell, A.S., 2001. Adenovirus E1A: remodelling the host cell, a life or death experience. Oncogene 20, 7824–7835. https://doi.org/10.1038/sj.onc.1204913

Garibaldi, A., Carranza, F., Hertel, K.J., 2017. Isolation of Newly Transcribed RNA Using the Metabolic Label 4-Thiouridine, in: Shi, Y. (Ed.), MRNA Processing, Methods in Molecular Biology. Springer New York, New York, NY, pp. 169–176. https://doi.org/10.1007/978-1-4939-7204-3_13

Genoveso, M.J., Hisaoka, M., Komatsu, T., Wodrich, H., Nagata, K., Okuwaki, M., 2020. Formation of adenovirus DNA replication compartments and viral DNA accumulation sites by host chromatin regulatory proteins including NPM1. FEBS J 287, 205–217. https://doi.org/10.1111/febs.15027

Hancock, M.H., Crawford, L.B., Pham, A.H., Mitchell, J., Struthers, H.M., Yurochko, A.D., Caposio, P., Nelson, J.A., 2020. Human Cytomegalovirus miRNAs Regulate TGF-β to Mediate Myelosuppression while Maintaining Viral Latency in CD34+ Hematopoietic Progenitor Cells. Cell Host & Microbe 27, 104-114.e4. https://doi.org/10.1016/j.chom.2019.11.013

Hector, R.E., Nykamp, K.R., Dheur, S., Anderson, J.T., Non, P.J., Urbinati, C.R., Wilson, S.M., Minvielle-Sebastia, L., Swanson, M.S., 2002. Dual requirement for yeast hnRNP Nab2p in mRNA poly(A) tail length control and nuclear export. The EMBO Journal 21, 1800–1810. https://doi.org/10.1093/emboj/21.7.1800

Hidalgo, P., Gonzalez, R.A., 2019. Formation of adenovirus DNA replication compartments. FEBS Lett 593, 3518–3530. https://doi.org/10.1002/1873-3468.13672

Janicke, A., Vancuylenberg, J., Boag, P.R., Traven, A., Beilharz, T.H., 2012. ePAT: A simple method to tag adenylated RNA to measure poly(A)-tail length and other 3' RACE applications. RNA 18, 1289–1295. https://doi.org/10.1261/rna.031898.111

Jenal, M., Elkon, R., Loayza-Puch, F., van Haaften, G., Kühn, U., Menzies, F.M., Vrielink, J.A.F.O., Bos, A.J., Drost, J., Rooijers, K., Rubinsztein, D.C., Agami, R., 2012. The Poly(A)-Binding Protein Nuclear 1 Suppresses Alternative Cleavage and Polyadenylation Sites. Cell 149, 538–553. https://doi.org/10.1016/j.cell.2012.03.022

Katahira, J., 2012. mRNA export and the TREX complex. Biochimica et Biophysica Acta (BBA) - Gene Regulatory Mechanisms 1819, 507–513. https://doi.org/10.1016/j.bbagrm.2011.12.001

Kim, Y.-J., Noguchi, S., Hayashi, Y.K., Tsukahara, T., Shimizu, T., Arahata, K., 2001. The product of an oculopharyngeal muscular dystrophy gene, poly(A)-binding protein 2, interacts with SKIP and stimulates muscle-specific gene expression. Human Molecular Genetics 10, 1129–1139. https://doi.org/10.1093/hmg/10.11.1129

Krause, S., Fakan, S., Weis, K., Wahle, E., 1994. Immunodetection of Poly(A) Binding Protein II in the Cell Nucleus. Experimental Cell Research 75–82.

Kruijer, W., Van Schaik, F.M.A., Speijer, J.G., Sussenbach, J.S., 1983. Structure and function of adenovirus DNA binding protein: Comparison of the amino acid sequences of the Ad5 and Ad12 proteins derived from the nucleotide sequence of the corresponding genes. Virology 128, 140–153. https://doi.org/10.1016/0042-6822(83)90325-2

Kühn, U., Gündel, M., Knoth, A., Kerwitz, Y., Rüdel, S., Wahle, E., 2009. Poly(A) Tail Length Is Controlled by the Nuclear Poly(A)-binding Protein Regulating the Interaction between Poly(A) Polymerase and the Cleavage and Polyadenylation Specificity Factor. Journal of Biological Chemistry 284, 22803–22814. https://doi.org/10.1074/jbc.M109.018226

Larsson, S., Svensson, C., Akusjärvi, G., 1992. Control of adenovirus major late gene expression at multiple levels. Journal of Molecular Biology 225, 287–298. https://doi.org/10.1016/0022-2836(92)90922-7

Leong, G.M., Subramaniam, N., Figueroa, J., Flanagan, J.L., Hayman, M.J., Eisman, J.A., Kouzmenko, A.P., 2001. Ski-interacting Protein Interacts with Smad Proteins to Augment Transforming Growth Factor-β-dependent Transcription. Journal of Biological Chemistry 276, 18243–18248. https://doi.org/10.1074/jbc.M010815200

Leong, K., Berk, A.J., 1986. Adenovirus early region 1A protein increases the number of template molecules transcribed in cell-free extracts. Proceedings of the National Academy of Sciences 83, 5844–5848. https://doi.org/10.1073/pnas.83.16.5844

Lillie, J.W., Loewenstein, P.M., Green, M.R., Green, M., 1987. Functional Domains of Adenovirus Type 5 E1a Proteins. Cell 50.

Liu, Y., Beyer, A., Aebersold, R., 2016. On the Dependency of Cellular Protein Levels on mRNA Abundance. Cell 165, 535–550. https://doi.org/10.1016/j.cell.2016.03.014

Logan, J., Shenk, T., 1984. Adenovirus tripartite leader sequence enhances translation of mRNAs late after infection. Proceedings of the National Academy of Sciences 81, 3655–3659. https://doi.org/10.1073/pnas.81.12.3655

Mann, K.P., Weiss, E.A., Nevins, J.R., 1993. Alternative Poly(A) Site Utilization during Adenovirus Infection Coincides with a Decrease in the Activity of a Poly(A) Site Processing Factor. Molecular and Cellular Biology 13, 9.

Meola, N., Domanski, M., Karadoulama, E., Chen, Y., Gentil, C., Pultz, D., Vitting-Seerup, K., Lykke-Andersen, S., Andersen, J.S., Sandelin, A., Jensen, T.H., 2016. Identification of a Nuclear Exosome Decay Pathway for Processed Transcripts. Molecular Cell 64, 520–533. https://doi.org/10.1016/j.molcel.2016.09.025

Moullec, J.M.L., Akusjarvi, G., Stalhandske, P., Pettersson, U., Chambraud, B., Gilardi, P., Nasri, M., Perricaudet', M., 1983. Polyadenylic Acid Addition Sites in the Adenovirus Type 2 Major Late Transcription Unit. J. VIROL. 48, 8.

Muniz, L., Davidson, L., West, S., 2015. Poly(A) Polymerase and the Nuclear Poly(A) Binding Protein, PABPN1, Coordinate the Splicing and Degradation of a Subset of Human Pre-mRNAs. Mol Cell Biol 35, 2218–2230. https://doi.org/10.1128/MCB.00123-15

Nakagawa, S., Ip, J.Y., Shioi, G., Tripathi, V., Zong, X., Hirose, T., Prasanth, K.V., 2012. Malat1 is not an essential component of nuclear speckles in mice. RNA 18, 1487–1499. https://doi.org/10.1261/rna.033217.112

Nanbo, A., Ohashi, M., Yoshiyama, H., Ohba, Y., 2018. The Role of Transforming Growth Factor β in Cell-to-Cell Contact-Mediated Epstein-Barr Virus Transmission. Front. Microbiol. 9, 984. https://doi.org/10.3389/fmicb.2018.00984

Neve, J., Patel, R., Wang, Z., Louey, A., Furger, A.M., 2017. Cleavage and polyadenylation: Ending the message expands gene regulation. RNA Biology 14, 865–890. https://doi.org/10.1080/15476286.2017.1306171

Palazzo, A.F., Lee, E.S., 2018. Sequence Determinants for Nuclear Retention and Cytoplasmic Export of mRNAs and lncRNAs. Front. Genet. 9, 440. https://doi.org/10.3389/fgene.2018.00440

Paul, B., Montpetit, B., 2016. Altered RNA processing and export lead to retention of mRNAs near transcription sites and nuclear pore complexes or within the nucleolus. MBoC 27, 2742–2756. https://doi.org/10.1091/mbc.e16-04-0244

Perreault, A., Lemieux, C., Bachand, F., 2007. Regulation of the Nuclear Poly(A)-binding Protein by Arginine Methylation in Fission Yeast. Journal of Biological Chemistry 282, 7552–7562. https://doi.org/10.1074/jbc.M610512200

Prescott, J., Falck-Pedersen, E., 1994. Sequence Elements Upstream of the 3' Cleavage Site Confer Substrate Strength to the Adenovirus Li and L3 Polyadenylation Sites. Molecular and Cellular Biology 14, 12.

Rädle, B., Rutkowski, A.J., Ruzsics, Z., Friedel, C.C., Koszinowski, U.H., Dölken, L., 2013. Metabolic Labeling of Newly Transcribed RNA for High Resolution Gene Expression Profiling of RNA Synthesis, Processing and Decay in Cell Culture. JoVE 50195. https://doi.org/10.3791/50195

Ramke, M., Lee, J.Y., Dyer, D.W., Seto, D., Rajaiya, J., Chodosh, J., 2017. The 5′UTR in human adenoviruses: leader diversity in late gene expression. Sci Rep 7, 618. https://doi.org/10.1038/s41598-017-00747-y

Reyes, E.D., Kulej, K., Pancholi, N.J., Akhtar, L.N., Avgousti, D.C., Kim, E.T., Bricker, D.K., Spruce, L.A., Koniski, S.A., Seeholzer, S.H., Isaacs, S.N., Garcia, B.A., Weitzman, M.D., 2017. Identifying Host Factors Associated with DNA Replicated During Virus Infection. Molecular & Cellular Proteomics 16, 2079–2097. https://doi.org/10.1074/mcp.M117.067116

Riba, A., Di Nanni, N., Mittal, N., Arhné, E., Schmidt, A., Zavolan, M., 2019. Protein synthesis rates and ribosome occupancies reveal determinants of translation elongation rates. Proc Natl Acad Sci USA 116, 15023–15032. https://doi.org/10.1073/pnas.1817299116

Rubio, M.A.T., Hopper, A.K., 2011. Transfer RNA travels from the cytoplasm to organelles: tRNA travels from the cytoplasm to organelles. WIREs RNA 2, 802–817. https://doi.org/10.1002/wrna.93

Salaun, C., MacDonald, A.I., Larralde, O., Howard, L., Lochtie, K., Burgess, H.M., Brook, M., Malik, P., Gray, N.K., Graham, S.V., 2010. Poly(A)-Binding Protein 1 Partially Relocalizes to the Nucleus during Herpes Simplex Virus Type 1 Infection in an ICP27-Independent Manner and Does Not Inhibit Virus Replication. J Virol 84, 8539–8548. https://doi.org/10.1128/JVI.00668-10

Schmid, M., Olszewski, P., Pelechano, V., Gupta, I., Steinmetz, L.M., Jensen, T.H., 2015. The Nuclear PolyA-Binding Protein Nab2p Is Essential for mRNA Production. Cell Reports 12, 128–139. https://doi.org/10.1016/j.celrep.2015.06.008

Sehgal, P.B., Darnell, J.E., Tamm, I., 1979. The Inhibition by DRB (5,6-Dichloro-1-/3-D- ribofuranosylbenzimidazole) of hnRNA and mRNA Production in HeLa Cells. Cell 9, 8.

Sehgal, P.B., Darnell, J.E., Tamm, I., 1976. The Inhibition by DRB (5,6-Dichloro-1-/3-D- ribofuranosylbenzimidazole) of hnRNA and mRNA Production in HeLa Cells. Cell 9, 8.

Shaw, A.R., Ziff, E.B., 1980. Transcripts from the adenovirus-2 major late promoter yield a single early family of 3′ coterminal mRNAs and five late families. Cell 22, 905–916. https://doi.org/10.1016/0092-8674(80)90568-1

Shi, M., Zhang, H., Wu, X., He, Z., Wang, L., Yin, S., Tian, B., Li, G., Cheng, H., 2017. ALYREF mainly binds to the 5′ and the 3′ regions of the mRNA in vivo. Nucleic Acids Research 45, 9640–9653. https://doi.org/10.1093/nar/gkx597

Simonelig, M., 2012. PABPN1 shuts down alternative poly(A) sites. Cell Res 22, 1419–1421. https://doi.org/10.1038/cr.2012.86

Smith, R.W.P., Gray, N.K., 2010. Poly(A)-binding protein (PABP): a common viral target. Biochemical Journal 426, 1–12. https://doi.org/10.1042/BJ20091571

Sonenberg, N., Hinnebusch, A.G., 2009. Regulation of Translation Initiation in Eukaryotes: Mechanisms and Biological Targets. Cell 136, 731–745. https://doi.org/10.1016/j.cell.2009.01.042

Spector, D.L., Lamond, A.I., 2011. Nuclear Speckles. Cold Spring Harbor Perspectives in Biology 3, a000646–a000646. https://doi.org/10.1101/cshperspect.a000646

Suzuki, K., Bose, P., Leong-Quong, R.Y., Fujita, D.J., Riabowol, K., 2010. REAP: A two minute cell fractionation method. BMC Res Notes 3, 294. https://doi.org/10.1186/1756-0500-3-294

Takagaki, Y., Manley, J.L., 1997. RNA recognition by the human polyadenylation factor CstF. Mol Cell Biol 17, 3907–3914. https://doi.org/10.1128/MCB.17.7.3907

Thomas, P.G., Mathews, M.B., 1980. DNA replication and the early to late transition in adenovirus infection. Cell 22, 523–533. https://doi.org/10.1016/0092-8674(80)90362-1

Tripathi, V., Ellis, J.D., Shen, Z., Song, D.Y., Pan, Q., Watt, A.T., Freier, S.M., Bennett, C.F., Sharma, A., Bubulya, P.A., Blencowe, B.J., Prasanth, S.G., Prasanth, K.V., 2010. The Nuclear-Retained Noncoding RNA MALAT1 Regulates Alternative Splicing by Modulating SR Splicing Factor Phosphorylation. Molecular Cell 39, 925–938. https://doi.org/10.1016/j.molcel.2010.08.011

Turtola, M., Manav, M.C., Kumar, A., Tudek, A., Mroczek, S., Krawczyk, P.S., Dziembowski, A., Schmid, M., Passmore, L.A., Casañal, A., Jensen, T.H., 2021. Three-layered control of mRNA poly(A) tail synthesis in *Saccharomyces cerevisiae*. Genes Dev. genesdev;gad.348634.121v1. https://doi.org/10.1101/gad.348634.121

Turunen, T.A., Roberts, T.C., Laitinen, P., Väänänen, M.-A., Korhonen, P., Malm, T., Ylä-Herttuala, S., Turunen, M.P., 2019. Changes in nuclear and cytoplasmic microRNA distribution in response to hypoxic stress. Sci Rep 9, 10332. https://doi.org/10.1038/s41598-019-46841-1

Wahle, E., 1995. Poly(A) Tail Length Control Is Caused by Termination of Processive Synthesis. Journal of Biological Chemistry 270, 2800–2808. https://doi.org/10.1074/jbc.270.6.2800

Wolf, E.J., Miles, A., Lee, E.S., Nabeel-Shah, S., Greenblatt, J.F., Palazzo, A.F., Tropepe, V., Emili, A., 2020. MKRN2 Physically Interacts with GLE1 to Regulate mRNA Export and Zebrafish Retinal Development. Cell Reports 31, 107693. https://doi.org/10.1016/j.celrep.2020.107693

Zhao, H., Chen, M., Pettersson, U., 2014. A new look at adenovirus splicing. Virology 456–457, 329–341. https://doi.org/10.1016/j.virol.2014.04.006